DETERMINATION OF THE TEMPERATURE RISE AND WRINKLING BEHAVIOR OF WEBS TRANSITING HEATED ROLLERS

By
RYAN OLIVER

Bachelor of Science in
Mechanical Engineering
Oklahoma State University
Stillwater, Oklahoma
2009

Submitted to the Faculty of
the Graduate College of the
Oklahoma State University
in partial fulfillment of
the requirements for
the Degree of
MASTER OF SCIENCE
May, 2014

DETERMINATION OF THE TEMPERATURE RISE

AND WRINKLING BEHAVIOR OF WEBS

TRANSITING HEATED ROLLERS

Thesis Approved:

Dr J K Good

Thesis Adviser

Dr H Hatami-Marbini

Dr G Young

ACKNOWLEDGEMENTS

I would like to thank my advisor, Dr James K Good, whose knowledge and experience was always able to provide guidance and understanding. I learned something new in almost every conversation we ever had. Working with him was both an honor and a privilege.

I would like to thank Mr Ron Markum, whose experience and intuition in the laboratory saved me countless hours of frustration and wasted effort.

I would like to thank my committee members, Drs, Hatami and Young, for their time and understanding. Their insight helped me look at things from a different perspective and better understand my own work.

I would like to thank my friends and loved ones. For being encouraging when I needed it. For helping me relax in times of frustration. And for being patient and understanding when I was consumed by my research and course work.

Lastly, I would like to thank the WHRC and its sponsors without whom my research would not have been possible.

Name: RYAN OLIVER

Date of Degree: MAY, 2014

Title of Study: DETERMINATION OF THE TEMPERATURE RISE AND WRINKLING BEHAVIOR OF WEBS TRANSITING HEATED ROLLERS

Major Field: MECHANICAL ENGINEERING

Abstract:

Many materials are manufactured and processed as webs. Examples of webs include: paper, plastic films, textiles, and metal foils. Due to the thin nature of webs, geometric instabilities can arise during web handling processes. These instabilities can cause the web to deform out of plane. When these deformations occur in the span between rollers, they are referred to as troughs. A wrinkle is any out of plane deformation that transits a roller along with the web. Wrinkles can cause creasing and damage to the web material.

There are many observed and documented conditions that cause the formation of troughs and wrinkles. One condition which has been widely observed not yet widely investigated is wrinkling of webs transiting rollers which are either heated or cooled. There are many processes which require the web to be either heated or cooled so understanding the behavior of the web as it undergoes temperature changes associated with these processes is advantageous to manufacturers. This research focuses on polyester film. The goal is to better understand the behavior of webs which transit rollers of elevated temperature and, also, determine the conditions under which wrinkling can occur and see if these conditions can be predicted.

TABLE OF CONTENTS

LIST OF TABLES

Table Page

LIST OF FIGURES

Figure Page

Figure Page

CHAPTER I

INTRODUCTION

Many items are manufactured and processed as webs. A web is a material whose width and length are orders of magnitude greater than is its thickness. Most often webs are stored on wound rolls and are processed by passing the web material over cylindrical rollers through machinery for treatment. This method of transport of the material is commonly referred to as web handling. The web material is usually transported over the roller by applying a tensile force along the web's length and leaving the edges of the material free. The direction in which the driving force is applied and in which the web moves is commonly referred to as the machine direction (MD), while the direction perpendicular to this, along the web's width, is commonly referred to as the cross-machine direction (CMD) or transverse direction (TD).

Due to the thin nature of webs, geometric instabilities can arise during web handling processes. These instabilities can cause the web to deform out of the plane defined by the MD and CMD. When these deformations occur in the span between rollers, they are referred to as troughs. In the area of a trough, the CMD cross section of the web usually

appears parabolic or sinusoidal. Though they are not desirable, troughs are not usually detrimental to the web or web processing. Usually as the web approaches a roller the trough dissipates and the web transits the roller as a smooth cylindrical shell. In some cases, however, excessively large troughs can lead to the formation of wrinkles. A wrinkle is any out of plane deformation that transits a roller along with the web. Wrinkles are visible and can cause creasing and damage to the web material.

SCOPE OF RESEARCH

There are many observed and documented conditions that cause the formation of troughs and wrinkles. Some of these, which have been analyzed in earlier studies include, misalignment of a roller, tapering of a roller, nonlinear roller profiles, lateral movement of the web, web discontinuities and variation in web dimensions. One condition which has been widely observed not yet widely investigated is wrinkling of webs transiting rollers which are either heated or cooled. There are many processes (drying, coating, laminating, embossing, etc.) which require the web to be either heated or cooled so understanding the behavior of the web as it undergoes temperature changes associated with these processes is advantageous to manufacturers. This research will focus on polyester film to try and better understand the behavior of webs which transit rollers at elevated temperature and, also, determine the conditions under which wrinkling can occur and see if these conditions can be predicted through equations and modeling.

CHAPTER II

REVIEW OF LITERATURE

Some of the earliest work done regarding theory governing the lateral dynamics of webs travelling through process machines was completed by Shelton[14]. He studied the effects of steering due to the misalignment of a downstream roller. Through this he was able to determine slack edge criterion and establish principles of normal entry and zero internal moment. The principle of normal entry states that, if a series of parallel lines exist in the web, in the MD, these lines will tend to achieve perpendicularity with the downstream roller. These principles are still important in establishing boundary conditions for finite element and equations based solutions.

Many times in analysis, webs between rollers are treated as thin linear elastic plates while webs on rollers are often analyzed as thin cylindrical shells. It has been shown, by Timoshenko and Gere [8], using membrane analysis that the critical buckling stress required to form troughs in a free span is:

$$\sigma_{cr} = -\frac{\pi t}{a}\sqrt{\frac{E\sigma_x}{3*(1-\nu^2)}} \tag{2.1}$$

where,

$E - Modulous\ of\ Elasticity\ of the\ web$
$t - web\ thickness$
$\sigma_x - MD\ stress$
$\nu - poisson's\ ratio\ of\ web$
$a - Span\ length\ in\ the\ MD$

Good, Beisel and Yurtcu[15] were able to show that Eqn 2.21 provided a reasonable criterion for troughs of isotropic and orthotropic material. As previously stated, the cylindrical buckling stress can be used as an analog for the critical stress required to create wrinkles on a roller. Timoshenko and Gere [8] also proposed the critical axial stress required to buckle an unpressurized cylinder as:

$$\sigma_{cr} = \frac{-E * t}{\sqrt{3 * (1 - \nu^2)} * R} \tag{2.2}$$

where,

$E - Modulous\ of\ Elasticity\ of the\ web$
$t - web\ thickness$
$\sigma_x - MD\ stress$
$\nu - poisson's\ ratio\ of\ web$
$R - radius\ of\ roller$

Good, Kedl and Shelton[1] were able to show that Eqn 2.2 provided a reasonable criterion for wrinkling on rollers due to roller misalignment. Later, Good and Straughan[2] were able to show the same for wrinkling of polyester (PET) and polyethylene (PEN) on rollers due to twist. Therefore, Eqn 2.2 can be used as a reasonable buckling criterion.

Jones[16] presented a comprehensive look at the traction between the web and roller. This included discussion of the Knox-Sweeney equation:

$$h_o = 0.65 * R * \left[\frac{12 * \mu_a * V}{T}\right]^{\frac{2}{3}} \tag{2.3}$$

Where

$h_o - air\ film\ thickness$
$R - Radius\ of\ Roller$

$T - Line\ Tension$
$V - Line\ Speed$
$\mu_a - dynamic\ viscosity\ of\ air$

which describes the thickness of the entrained air layer that exists between the web and roller. Jones[16] also presented description of the steering and '*Normal Entry Rule*' which describes the tendency of webs to contact rollers perpendicular to the roller axis. Also, Jones[16] defines the maximum stress that can be supported by the frictional force between the web abs roller as:

$$\sigma_{y,max} = \frac{\mu\, T\, w}{2\, R\, t} \tag{2.4}$$

Where

$w - width\ of\ web$
$R - Radius\ of\ Roller$
$T - Line\ Tension$
$\mu - coefficient\ of\ friction$
$t - web\ thickness$

And states that is this value is greater than the critical buckling stress, wrinkling can occur.

There have been several studies about thermal effects and behavior of webs and rollers. Lightbourn[3] presented testing methods and results for determination of contact resistance between the web and roller. He then used these results with both lumped capacitance and finite difference methods to model temperature rise. These analytical models were then compared to experimental data points. While the contact resistances determined did seem to agree with experimental values, they were only determined on a case by case basis and disregarded the magnitude of the air film layer.

Jones, McCann and Abbott[7] used lumped capacitance to model temperature rise in a web. They then looked at how the thermal expansion

affects stress and strain in both the MD and CMD. The thermal expansion created areas of negative compressive stress. The expansion also created areas of micro slip between the web and roller which created gradients of stress and strain close to the contact boundaries. In Jones[7] analysis the aforementioned critical buckling stress was used a the criterion for wrinkling.

Later, Jones, McCann and Bishop[18} presented a thermally induced wrinkling model based on the assumption that a piece of particulate existed between the we bad the roller. This assumption arose because the model was based on a vacuum deposition process. In this process, the web transited a cooling roller while the outer surface was heated simultaneously by deposition of coating material. If a single piece of material existed between the web and roller then it would create a 'tent' in the web. As the web temperature increased the tent would increase in height until it separates from the particulate and becomes a wrinkle.

Pagilla and Lu[6] were able to apply separation of variables and eigenvalue principles to the basic heat equation, where

$$\frac{\partial \theta}{\partial \tau} = \kappa \frac{\partial^2 \theta}{\partial y^2} \tag{2.5}$$

becomes

$$\frac{Y''}{Y} = \frac{T'}{\kappa T} \tag{2.6}$$

With the solutions

$$T(\tau) = e^{-\lambda^2 \kappa \tau}$$
$$Y(y) = A\cos(\lambda y) + B\sin(\lambda y) \tag{2.7}$$

$\lambda - eigenvalues\ of\ the\ system$

From there, using Fourier expansion and summation, a 1-D model of temperature distribution of a web transiting a heated roller was derived. Their model was able to account for conduction and convection to the web under multiple conditions. This included convection in free span areas where the web is between rollers and in areas of web-roller contact. This model will be used in later sections to compare experimental data to measured data.

The majority of work by Jones[7,16,18] was analytical in nature. While both Lightbourn[3] and Lu[6] compared their models to experimental data, they did not take many data points in areas where the web was in contact with the roller. In both cases, temperature measurements were taken upstream and downstream of the heated rollers. This means that the actual temperature profile on the roller was unknown.

RESEARCH OBJECTIVE

The objective of this research is to use testing to determine the characteristics of the temperature rise of the webs transiting a heated roller and compare these results to analytical heat transfer models. Also, this research will focus on conditions under which temperature increase causes wrinkles to be generated on the roller. In the case of wrinkling, FEA modeling will also be used to determine the stresses which develop under conditions under which wrinkles do and not occur. This research is unique in that no earlier studies appear to use experimental data to determine temperature rise and temperature driven wrinkling conditions.

CHAPTER III

TEMPERATURE RISE EXPERIMENTS: SETUP & RESULTS

The first experiments in this research were completed to determine the temperature rise of webs transiting heated rollers and observe if any wrinkling would occur. Web line operating parameters were varied to observe their impact on the temperature rise.

MATERIAL/EQUIPMENT

The web material used for the temperature rise testing consisted of 0.002 inch thick (200 gage) by 6 inch wide translucent polyester web. Polyester (polyethylene terephthalate - PET) was chosen because it is isotropic as well as linear elastic in nature and many of its properties are not greatly impacted by temperature change[10].

Initially, the web was processed using a wind/unwind system as seen in the following figure. The roll of PET was placed on an unwind roller, run over several idler rollers, through a web guide, across the heated roller and then to a winding roller. The unwind roller was attached to an electro-magnetic braking system. The unwinding roller was used to control the line tension of the system. A roller supported by a load cell provided a web tension, which was used to provide feedback to the electromagnetic brake.

The winding roller was driven by an electric motor, varying angular velocity of the winder controlled the line speed of the system. It can be seen in the figure that the wrap angle of the web around the heated roller is slightly greater than 180 degrees.

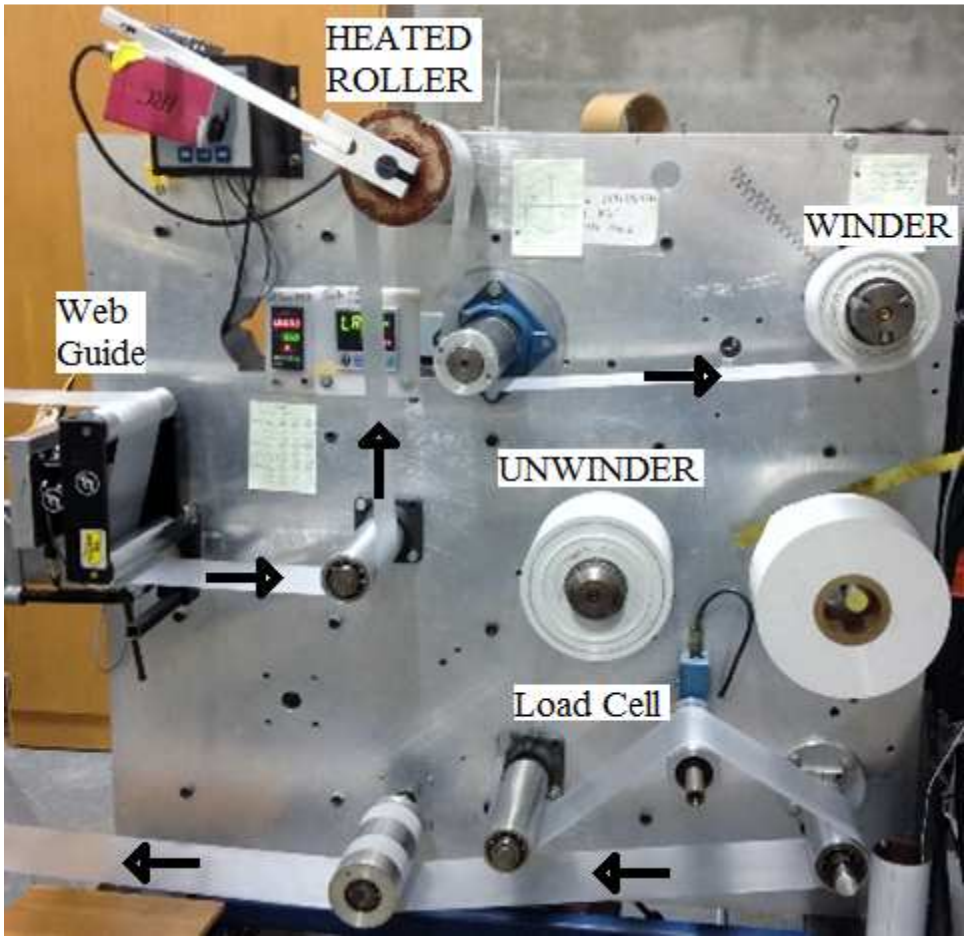

Figure 1 Web Path and Equipment Layout

HEATED ROLLER

In order to heat the PET, an internally heated roller was used. For the temperature rise experiments the roller was internally heated by an oil bath that was heated by an electric heating element. The roller consists of a hollow aluminum cylinder, capped on the ends with aluminum plates which were press-fit into place. The outer diameter of the heated roller is ~5.51

inches. A semi-hollow fixed steel shaft passed through roller bearings mounted in the plates.

Figure 2 Heated Roller Heating Element

Figure 3 Roller Shell

Figure 4 Roller Cap and Bearings

Wires, passed through the center of the hollow shaft, were connected to a heating element which was mounted in a nylon block. The roller was filled almost halfway with quenching oil so that when the heating element was below the shaft, it was submerged in the quenching oil. The temperature of the aluminum roller was determined by controlling the current passed through the heating element which in turn heated the oil.

The temperature of the oil was maintained using a PID controller. The controller used a type J thermocouple, which was also passed through the center of the shaft and submerged in the oil bath, to provide temperature feedback. The controller used a solid state relay to control current supplied to the heating element.

TEMPERATURE MEASUREMENT

Temperature data was recorded using both thermocouples and an infrared (IR) thermometer. The thermocouples utilized for these experiments were designed to measure the temperature of moving surfaces. Each had a spring loaded detection head with a type K thermocouple. The spring determined the pressure between the detection head and the surface to be measured.

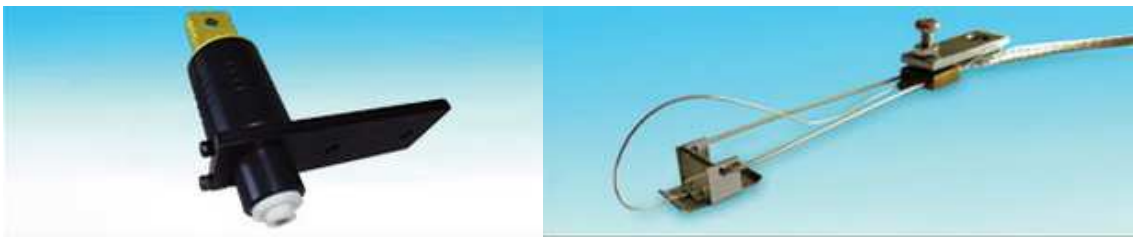

Figure 5 Thermocouples used to take Surface Readings

Air temperature in these experiments was measured using a basic type K thermocouple suspended in air, close to the material surface, upstream of the heated roller. It was assumed for all experiments that the material entering the free span before the heated roller was equal to the air temperature of the laboratory. This assumption was made based on the fact that all of the idler rollers in the system were at room temperature at the

start of the experiments. In nearly all cases the room temperature was found to be ~72 ˚F.

During a majority of the testing, an infrared thermometer was utilized as well. The infrared thermometer used was designed specifically to measure the temperature of polyester webs. It has been found that at a wavelength of 7.9 micrometers, polyester does not transmit radiation energy through its thickness[13]. Therefore, a thermometer was acquired which was tuned to a 7.9 micrometer wavelength. This allowed for the surface temperature of the polyester to be recorded without interference from the heated roller.

Figure 6 Infrared Thermometer and Controller

DATA RECORDING

The thermocouple output data was recorded digitally. All thermocouples were plugged into a 4-channel data logger. Readings were taken at one second intervals. Data was then transferred, in real time, via USB, to a PC and recorded to a text file so an average value could be determined later.

For the IR data, the thermometer was connected to a controller/display. Then data was transmitted via 4-20 milliamp signal to an analog data card connected to a PC. Readings were taken at 3 millisecond intervals and then recorded and averaged using Lab-View. The average values were saved as data files.

ROUND 1: TEST SETUP

Initially, two thermocouples were attached to a bar that was attached to a block mounted on the heated roller's central shafts seen in the figure below. This allowed the block to be rotated so that readings could be taken at different locations while maintaining distance and tangential orientation of the thermocouple relative to the roller. Rotating the block changed the position of the thermocouple in the machine direction while sliding the thermocouple on the bar changed the position in the cross machine direction.

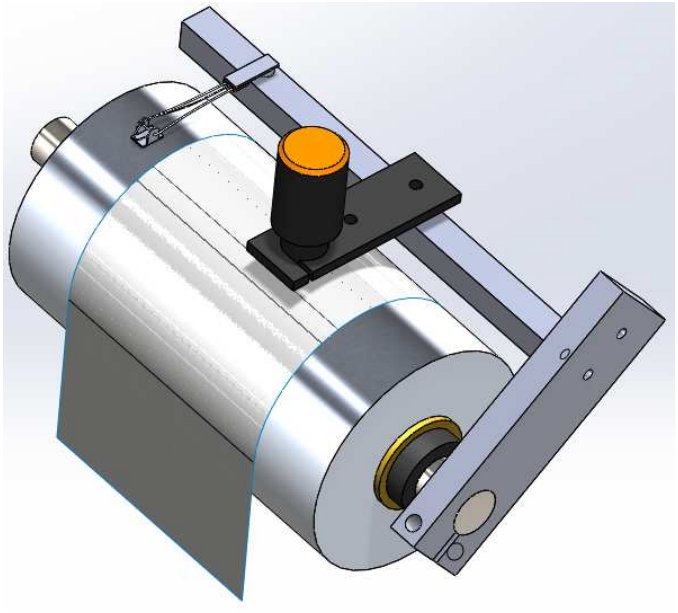

Figure 7 Thermocouple Roller Test Setup

The roller internal oil bath temperature was set so that the surface temperature of the roller reached roughly 95 °F. This usually required an oil temperature of roughly 105 °F. The material temperature was recorded using a grid system, shown below, formed by 35 points. This grid consisted of 7 positions in the CMD and 5 positions in the MD. The CMD positions were spaced at 1.0 inch and 0.5 inch intervals and centered on the web centerline. The MD positions were spaced at 10 degree rotational intervals. The point where the web and the heated roller came into contact was considered the 0 degree position. For each position for which web temperature data was recorded, roller surface temperature and air temperature were also recorded. Roller and air temperature data were both recorded with type K thermocouples.

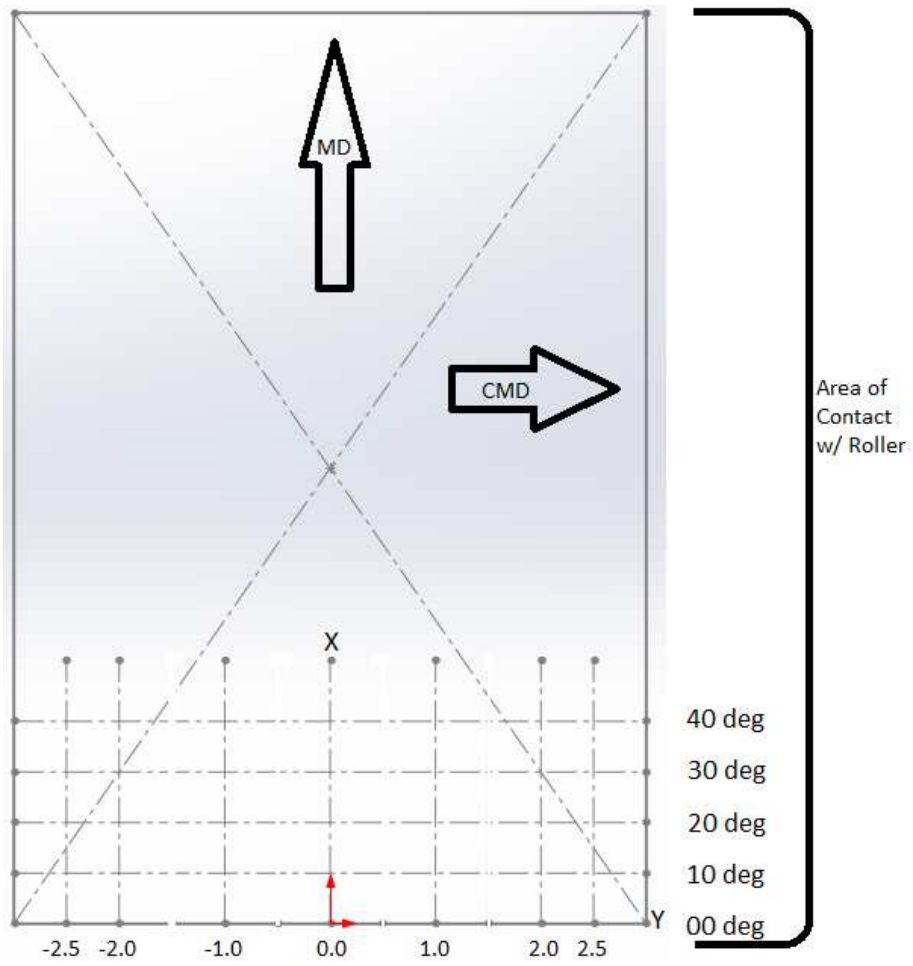

Figure 8 Round 1 Reading Locations

For the very first round of experiments, the web line speed was set as 75 feet per min (FPM). The line tension was set to 1 pound-force per linear inch (PLI) of web width. This meant the total force, for a 6 inch wide web, was 6 pounds force.

ROUND 1: PROCEDURE

The experimental procedure was a follows. The system was allowed to come to steady state (i.e., line speed, line tension and roller surface temperature reached desired values and remained constant). The thermocouples were rotated to the 0 degree position and readings were

taken at each of the CMD positions. At each location, once the thermocouple readings had reached steady state, temperature data was recorded over a 3 minute span. Roller surface temperature, air temperature and material temperature data was recorded simultaneously. Once data had been taken at all CMD positions for a given MD position, the thermocouple was rotated 10 degrees in the MD and the process was repeated. This was done for the 0-40 degrees MD range. 40 degrees appeared sufficient since the web temperature seemed to reach 99% of the roller surface temperature at that location.

ROUND 1: RESULTS

The temperature vs. position data for the first round of experiments is shown below. It can be observed that the data appears to be parabolic in nature. It can also be observed that the measured web temperature at entry were above the measured air temperature. Also of note, there appeared to be no noticeable gradient in temperature in the CMD at a given MD position. It should be noted as well that no wrinkles were observed during these experiments.

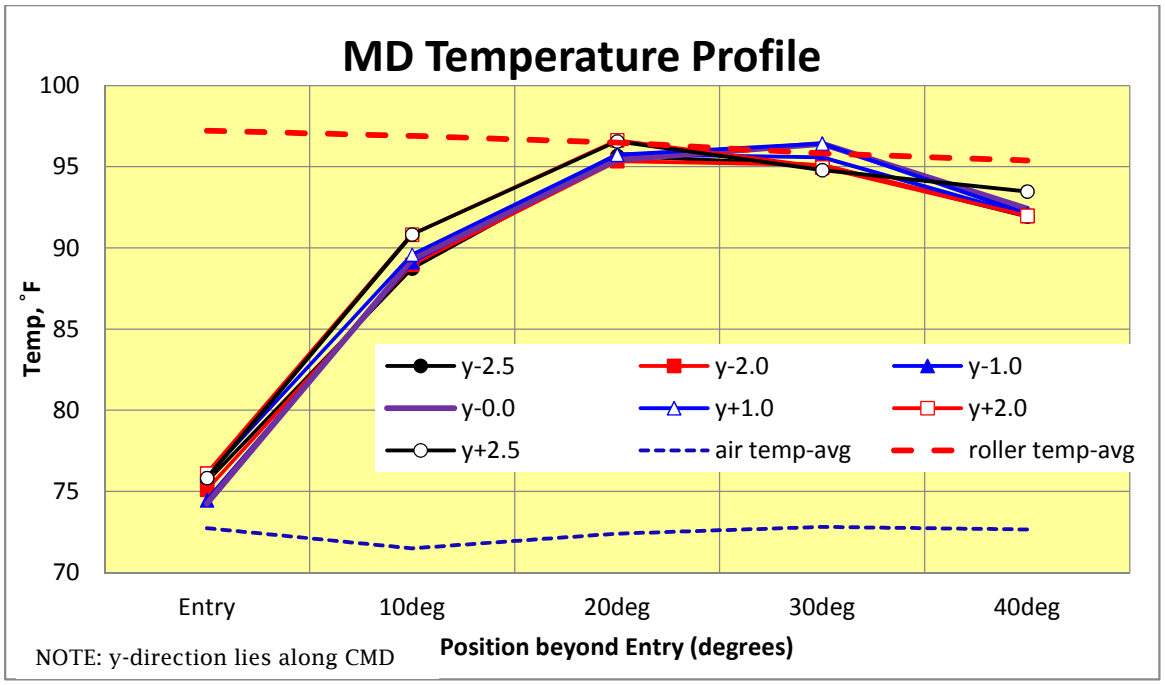

Figure 9 Round 1 Temperature Profile

After the initial experiments, a few issues were noticed while recording data with the thermocouples. First, it was sometimes difficult to maintain proper contact between the thermocouple and the PET. Also, the thermocouples would sometimes score the web. Lastly, it was realized that the contact pressure introduced by the thermocouple spring loaded head altered the interactions of the roller and the PET. It is known that as a web starts to transit a roller, a thin layer of air becomes trapped between the web and the roller. Therefore the extra pressure from the thermocouple would artificially decrease the air film layer and increase the contact area between the PET and the roller. This would not properly reflect conditions which would exist in a standard manufacturing environment. After these realizations the aforementioned IR thermometer was attained. This allowed for temperature measurements to be taken without affecting the results at the point of measurement.

ROUND 2: PROCEDURES

In the second round of experiments, line speed and tension were varied to observe their effect on temperature rise of the web. Line tension would be set at between 1, 2, and 3 PLI. Line speed would be set at 75, 150 and 225 FPM. This created 9 scenarios to be recorded and compared.

Also for these experiments, only an infrared thermometer would be used to record the web temperature. The roller and air temperatures would continue to be recorded using thermocouples. The IR thermometer was mounted in a manner similar to the thermocouple. The main difference being that the IR thermometer lens needed to be roughly 8 inches from the material to minimize the focal area and increase accuracy. The thermocouple used to measure the roller surface was mounted on the block that held the heated roller in place.

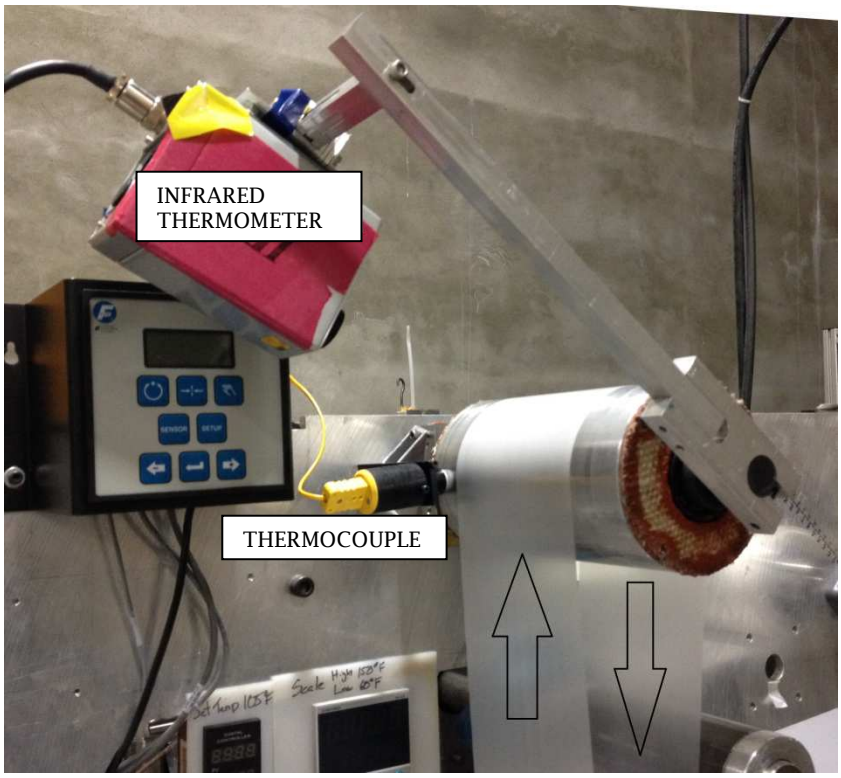

Figure 10 Infrared Testing Configuration

The temperature measurement procedure for the second round of experiments was similar to the first except for a few points. Data would be recorded at 3 CMD positions instead of 7: the material centerline (y= 0.0) and 0.5 inches inbound of the edges (y= ±2.5 inches). Data recordings would be taken at 10 degree intervals in the MD until the temperature appeared to reach an asymptotic value. In most cases, this only required data to be recorded from 0 - 90 degrees. Data would be recorded for a period of 3 minutes to determine an average temperature at each location.

ROUND 2: RESULTS

The following plots resulted from the second round of experiments. The first plots are grouped to show the impact of varying velocity on the behavior of the temperature rise. Therefore in these plots, tension is

constant for all data points. These plots are temperature vs. time plots. Time is measured in seconds and is the amount of time the web and roller are in contact. At 75 FPM a single point in the web takes ~0.58 seconds to transit the heated roller. The second set of plots is grouped to show the impact of varying tension on the behavior of the temperature rise.

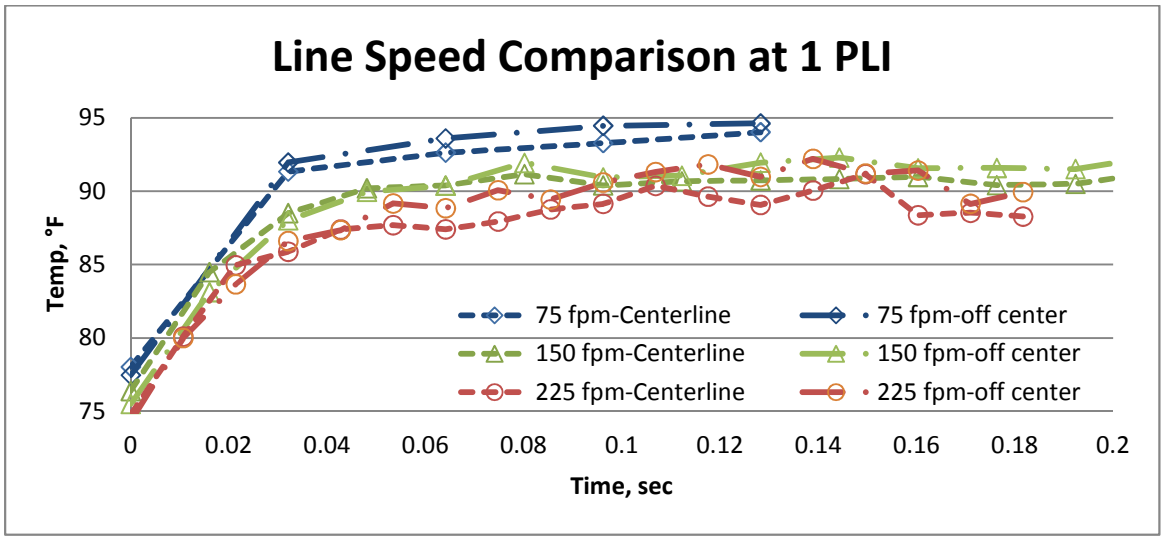

Figure 11 Round 2, 1 PLI, Temperature Rise

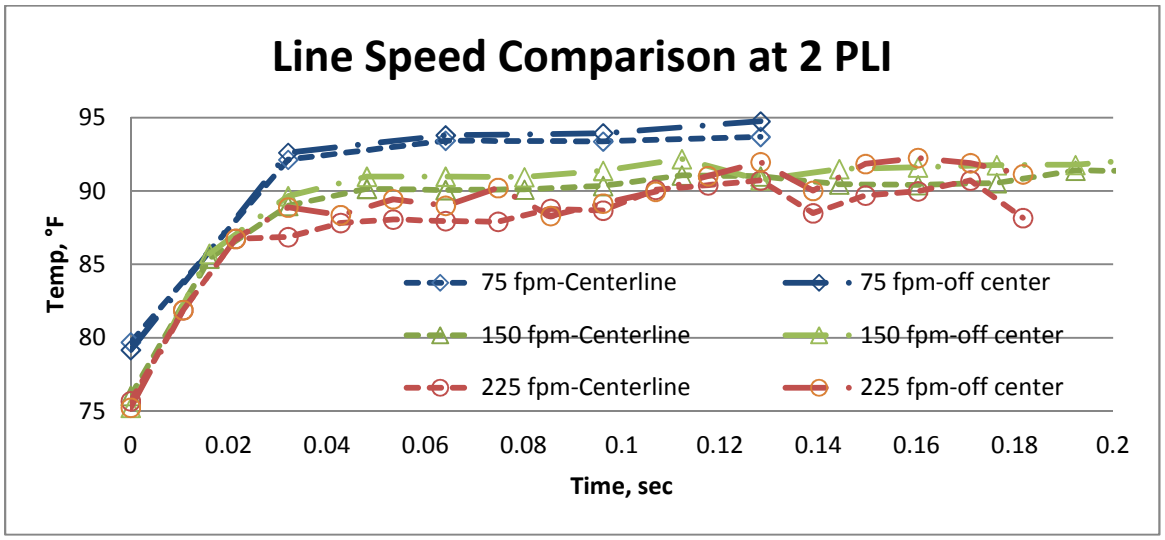

Figure 12 Round 2, 2 PLI, Temperature Rise

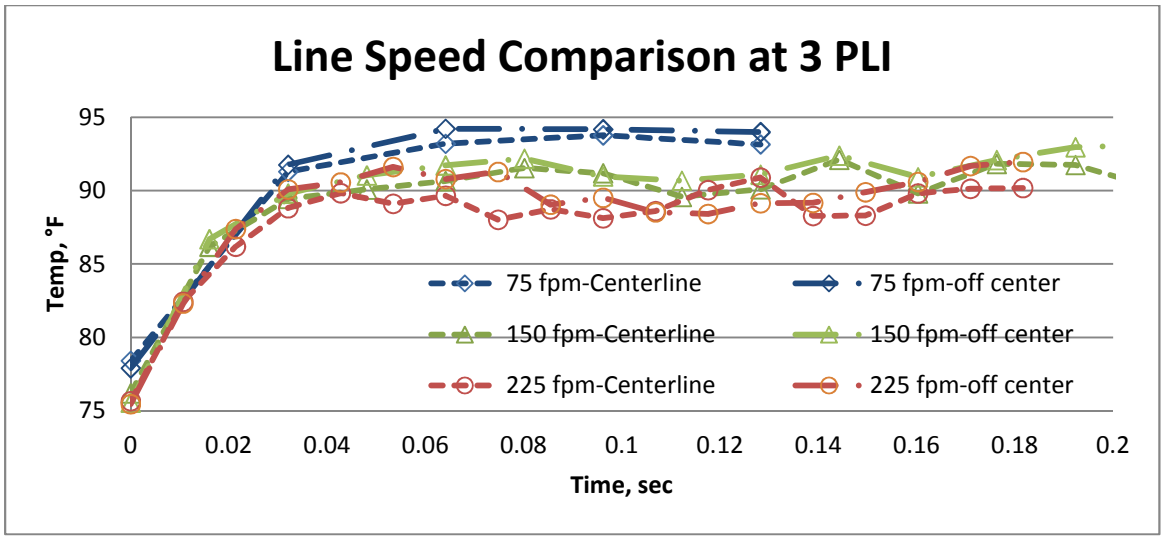

Figure 13 Round 2, 3 PLI, Temperature Rise

It can be seen in the plots above that as line speed increases the asymptotic value of the temperature rise decreases. This is likely partially due to the effect of air entrainment. As previously mentioned, it is known that an air fluid film forms between the web and roller. The thickness of this air film layer is given by[9]:

$$h_o = 0.65 * R * \left[\frac{12 * \mu * V}{T}\right]^{\frac{2}{3}} \tag{3.1}$$

Where

$h_o - air\ film\ thickness$
$R - Radius\ of\ Roller$
$T - Line\ Tension$
$V - Line\ Speed$
$\mu - dynamic\ viscosity\ of\ air$

Per Eqn (3.1), as velocity increases, and tension decreases, the thickness of the air film layer increases. This would reduce heat transfer via conduction between the roller and web.

It can also be observed that the lowest line speed, the temperature at the entry point is noticeably higher than room temperature. This is possibly

due to the effects of radiation and convection coming off the heated roller acting on the web in the entry span.

The following plots show the effects of varying tension at a constant line speed:

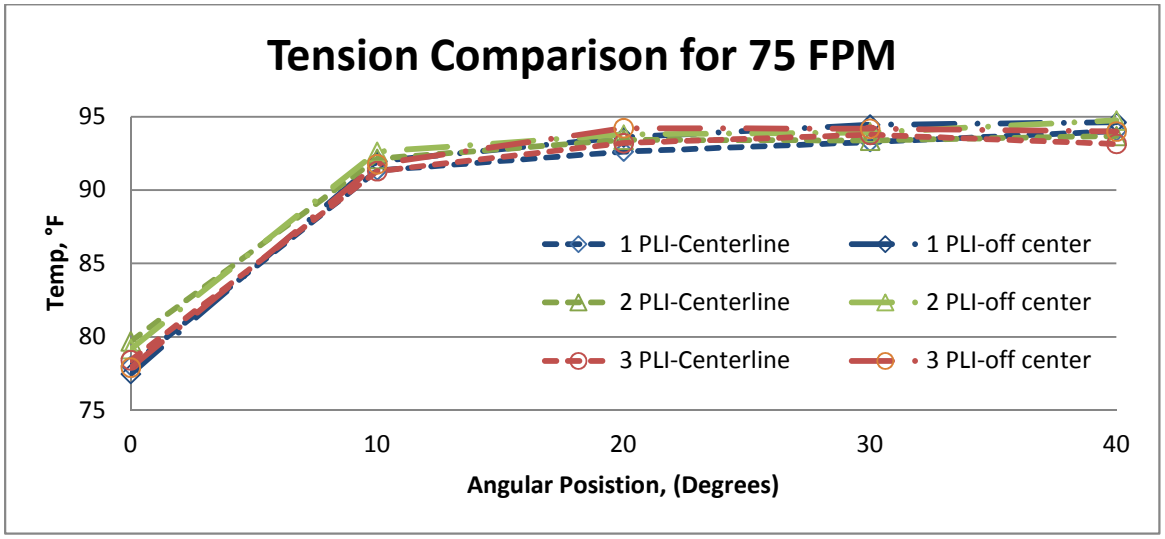

Figure 14 Round 2, 75 FPM, Temperature Rise

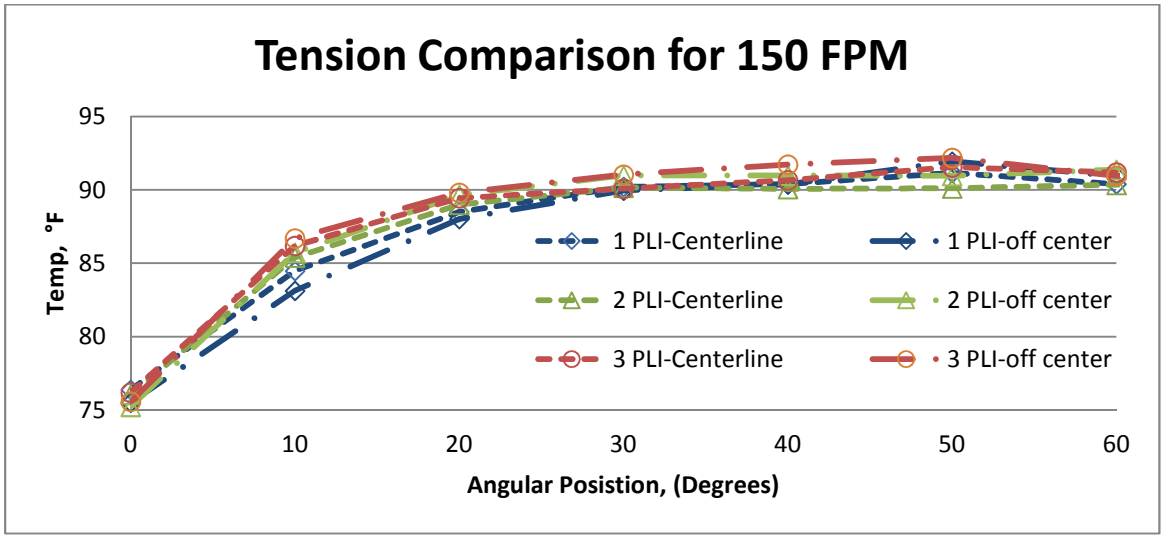

Figure 15 Round 2, 150 FPM, Temperature Rise

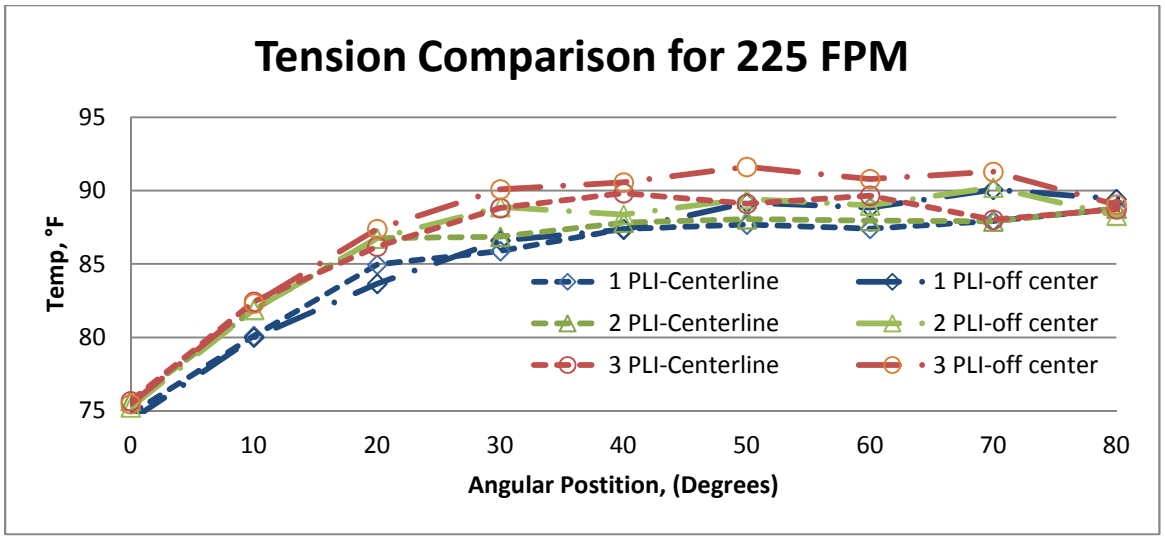

Figure 16 Round 2, 225 FPM, Temperature Rise

It can be seen in the preceding plots that the web temperature increases with line tension increase and line speed decrease. This is apparent at the 10 and 20 degree positions. The spread of the data is greater in the 150 FPM plot than the 75 FPM plot, and greater in the 225 PFM plot than the 150 FPM plot. It can also be seen in the 150 and 225 PFM plots that as tension increases the rate of temperature change increases as well. This agrees with the Knox-Sweeney equation since, as tension increases at a given velocity, the air film layer decreases creating greater contact area between the web and roller.

In all of the graphs for the ROUND 2 experiments, the initial segment of the temperature rise approaching the asymptotic value appears almost linear. This is unexpected since in most heat transfer problems, the temperature rise resembles continuous power functions in time. In order to better define the temperature rise, the ROUND 2 experiments were repeated with more data points added in the 0-20 degree positional range. It should

be noted that no wrinkles were generated due to temperature change during the ROUND 2 experiments.

ROUND 3: PROCEDURES

In the ROUND 3 experiments, additional data points were taken at 2.5, 5.0 and 15 degree MD locations. These experiments were also taken using a belt system in lieu of a wind/unwind system. Use of a belt system allowed for better control of line speed. It also allowed for steady state of the system to be maintained for longer periods of time. In the belt system, a ribbon of PET of fixed length is spliced into a continuous loop. Then the belt is passed over the idler rollers and driven roller, as well as a spring loaded "dancer" roller. Once again, varying the angular velocity of the driven roller controls the line speed. In the belt system, the line tension is controlled by changing the deflection of the springs attached to the dancer roller. Tension was measured using the same load cell as the first 2 rounds of experiments. Aside from these changes, the procedures for the 3rd round of experiments were identical to the second.

ROUND 3: RESULTS

The following plots are from third round of experiments. Once again, the first plots are grouped to show the impact of varying velocity on the behavior of the temperature rise. The second plots are grouped to show the impact of varying tension on the behavior of the temperature rise. In all the plots, the average value of the measurements at each MD location was used.

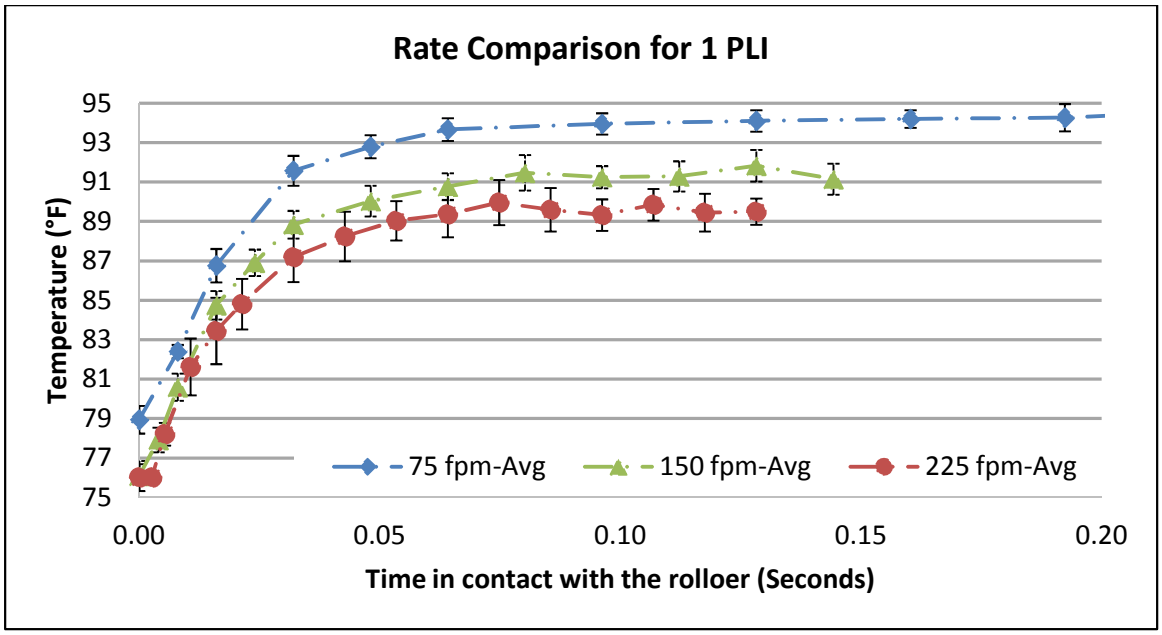

Figure 17 Round 3, 1 PLI, Temperature Rise

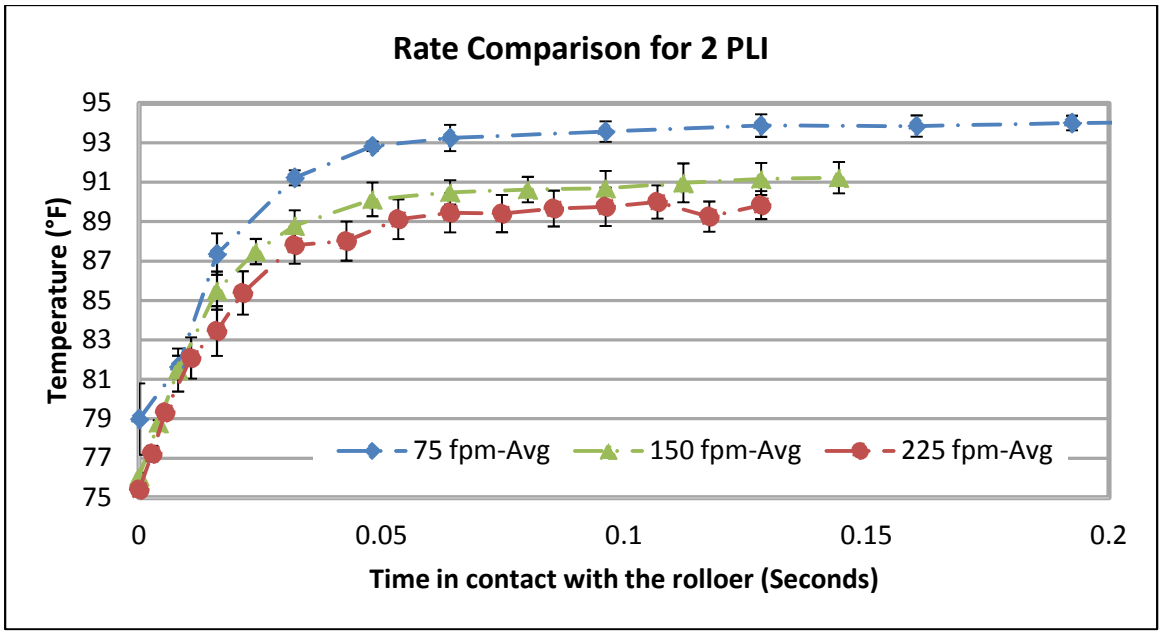

Figure 18 Round 3, 2 PLI, Temperature Rise

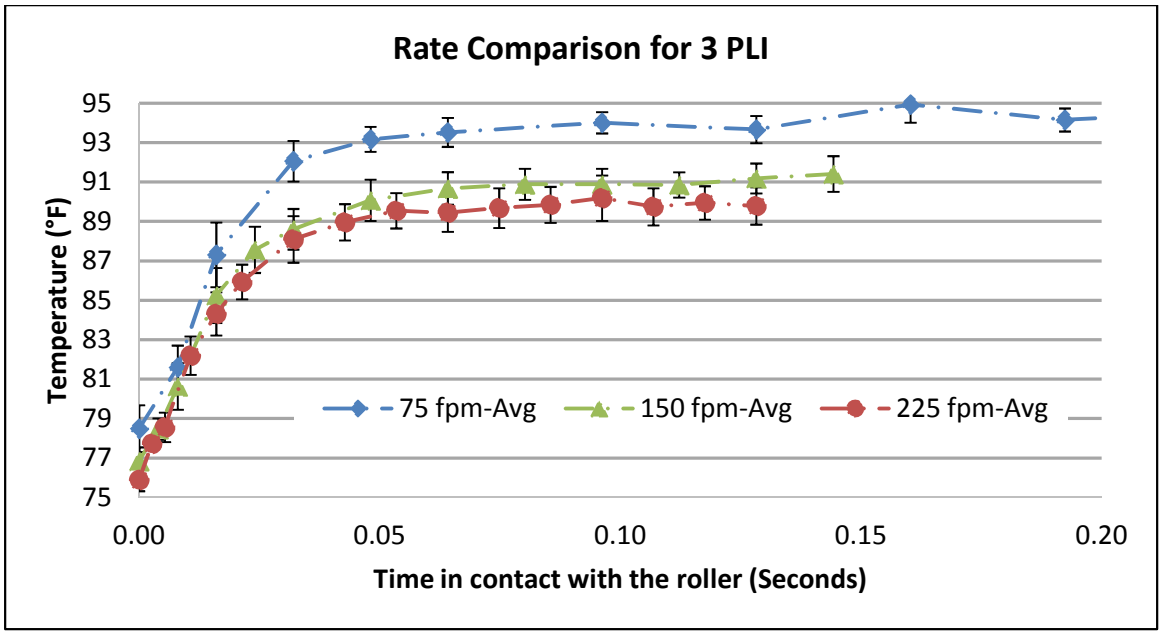

Figure 19 Round 3, 3 PLI, Temperature Rise

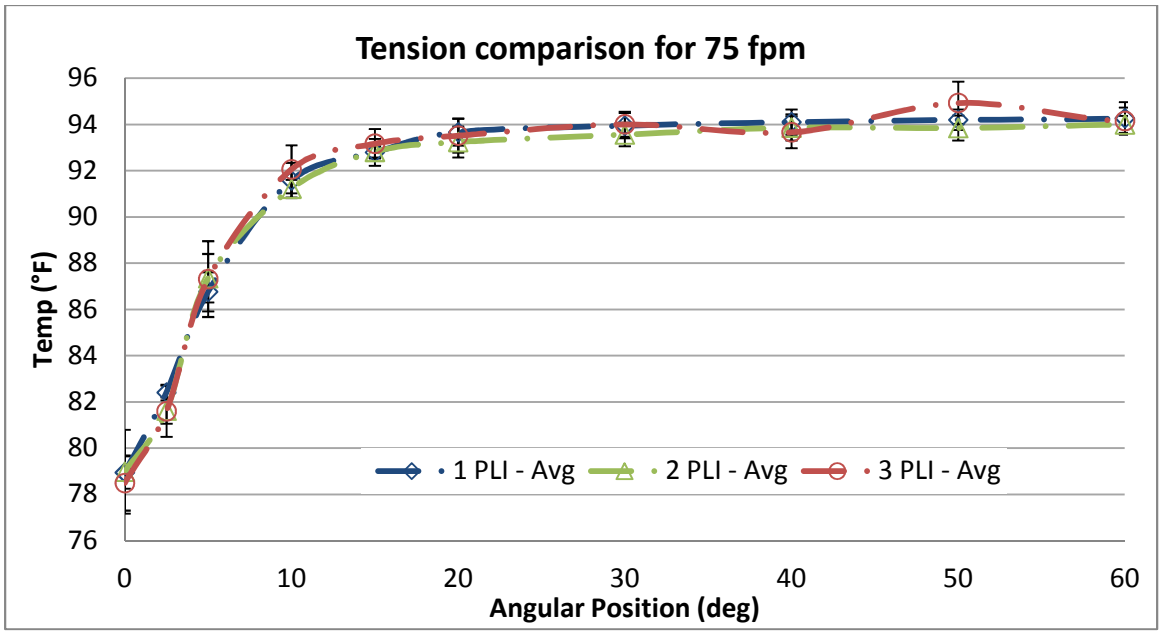

Figure 20 Round 3, 75 FPM, Temperature Rise

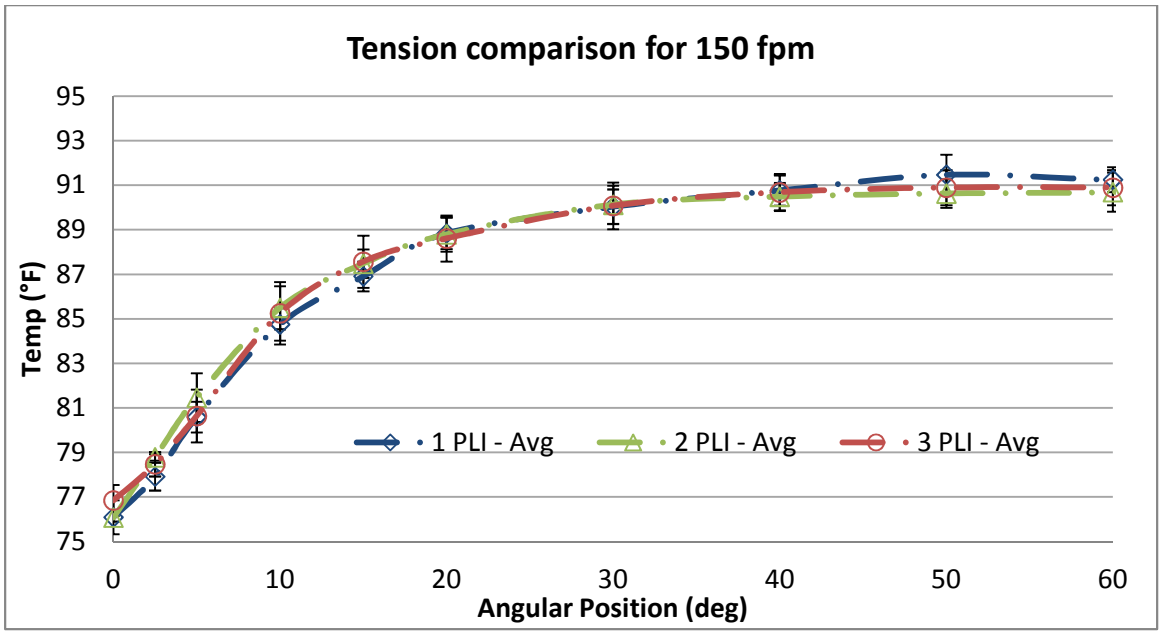

Figure 21 Round 3, 150 FPM, Temperature Rise

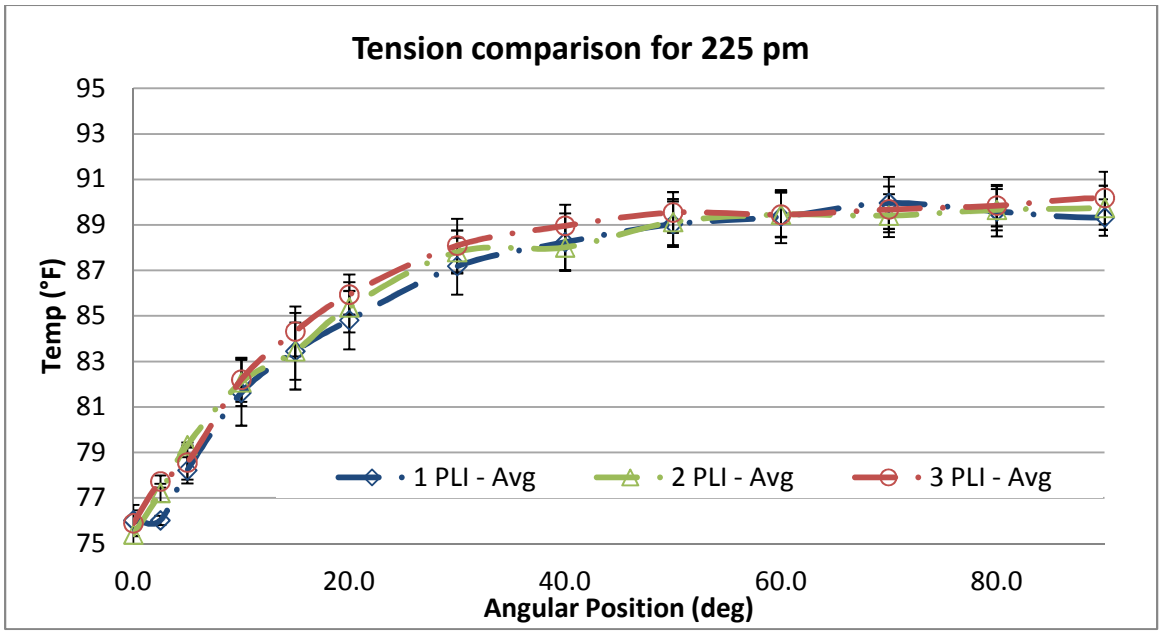

Figure 22 Round 3, 225 FPM, Temperature Rise

It can be seen in the plots above that the same trends that existed in the round 2 results exist in the round 3 results. The additional points in the 0-20 degree position range show that the temperature rise resembles a power function, which is expected of most heat transfer conditions.

CHAPTER IV

MODELING THE TEMPERATURE RISE

In the following chapter, the experimental temperature rise data will be compared to analytical solutions. The first, a basic 1-dimensional model was created using finite elements. Also, an analytical model was developed using finite difference method. Finally, a model was created based on of the solution found by Pagilla and Lu[6]. In all of these models, perfect conduction was assumed between the web and the roller. Doing this neglects the effects of air entrainment and thermal contact resistance. The material properties of the PET used in these models are shown below. These material properties were taken from reference material provided by the manufacturer[10].

Table 1 Thermal Properties of Polyester

Property	**Value**	**Units**
Thermal Conductivity, k	0.001548	W/(cm-degC)
Specific Heat, c	1.6284	J/(cm^3-degC)
Mass Density, ρ	1.39	g/ cm^3
Thickness, h	0.00508	cm

The first model utilized finite element methods (FEM) [11]. Specifically the Galerkin method coupled with finite difference equations via the following:

$$([C] + \theta[K]\Delta t)\{\Phi\}_b = ([C] - (1-\theta)[K]\Delta t)\{\Phi\}_a + \Delta t\big((1-\theta)\{F\}_a + \theta\{F\}_b\big) \quad (4.1)$$

Where
$[C] - capacitance\ matrix$
$[K] - conductance\ matrix$
$\theta = \frac{2}{3}\ for\ Galerkin\ method$
$\Delta t - time\ step, = 0.005\ sec$
$\{\Phi\}_a - nodal\ values\ at\ a\ on\ the\ interval\ [a, b]$
$\{\Phi\}_b - nodal\ values\ at\ b\ on\ the\ interval\ [a, b]$
$\{F\}_a = \{0\}, heat\ flux\ at\ a$
$\{F\}_b - \ heat\ flux\ at\ a$

The web thickness was divided into four segments through the thickness of the web and created 16 time steps within the time it takes a single point to transit the heated roller. The surface node data was plotted against the experimental data. The effect of convection was neglected at the surface node to simplify model and because convection coefficient was unknown.

The second analytical model was based on explicit finite difference methods (FDM). The FDM model used 5 nodes. The explicit FDM model determines the future values of a nodal temperature base on past known values. Node 0 was considered the roller contact node and was given a constant temperature at every time step. Node 4 was considered the surface node. Once again the effect of convection was neglected at the surface node. Equations for the FDM are shown below.

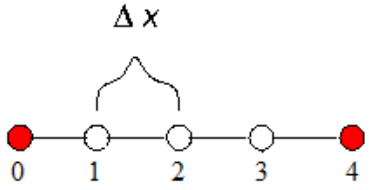

Figure 23 Finite Difference Nodal Model

For Node 0, the temperature at all steps

$$T_0^p = T_\infty \ , \qquad p - current\ time\ step, \qquad T_\infty - asymptotic\ temperature \tag{4.2}$$

For interior nodes, the temperature of node, m, at step, p+1, is

$$T_m^{p+1} = Fo * \left(T_{m+1}^p + T_{m-1}^p\right) + (1 - 2 * Fo) * T_m^p \tag{4.3}$$

where

$$Fo = \frac{\alpha * \Delta t}{(\Delta x)^2} \tag{4.4}$$

$\Delta x = 0.005\ in, \qquad distance\ between\ nodes\ through\ web\ thickness$
$\Delta t = 0.0002\ sec, \quad largest\ time\ step\ that\ keeps\ method\ stable$

$$\alpha = \frac{k}{\rho c} \tag{4.5}$$

$k - thermal\ conductivity$
$c - specific\ heat$
$\rho - density$

For the surface node, Node 4, the temperature is

$$T_5^{p+1} = 2 * Fo * \left(Bi * T_\infty + T_4^p\right) + (1 - 2 * Fo - 2 * Fo * Bi) * T_5^p \tag{4.6}$$

Since the effects of convection were neglected $Bi = 0$.

The following plots show both FEM and FDM models vs. the experimental data. In each case the target temperature for the FEM and FDM models were set to the maximum experimentally measure value instead of the roller surface temperature. The values plotted are the values of the surface nodes.

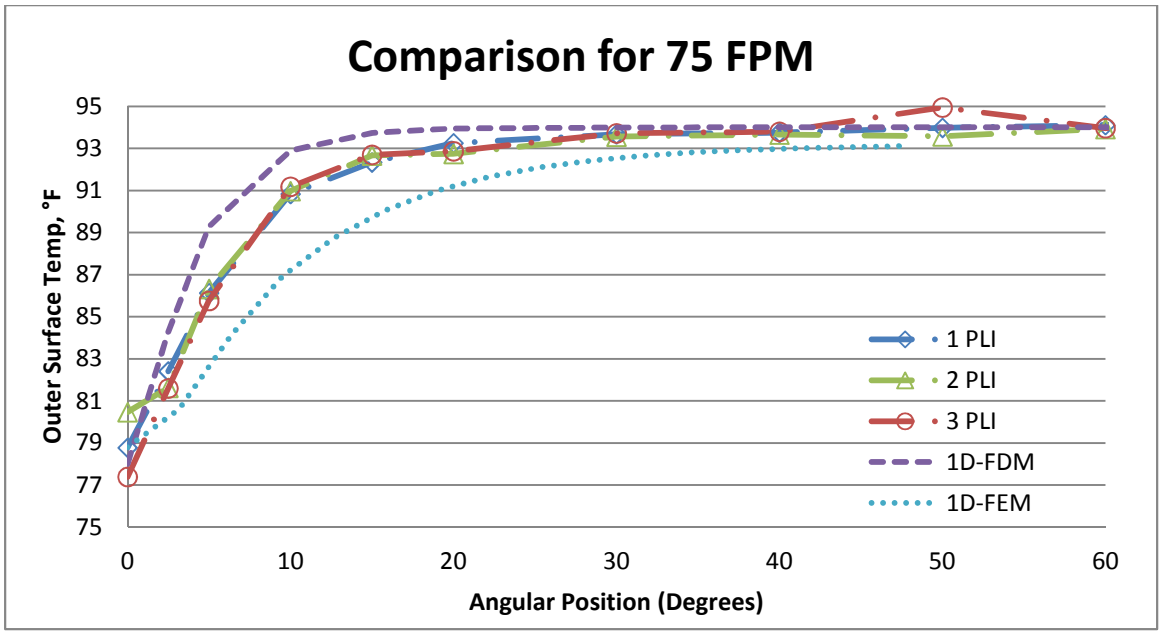

Figure 24 Comparison of FEA and FDM to Test Data, 75 FPM

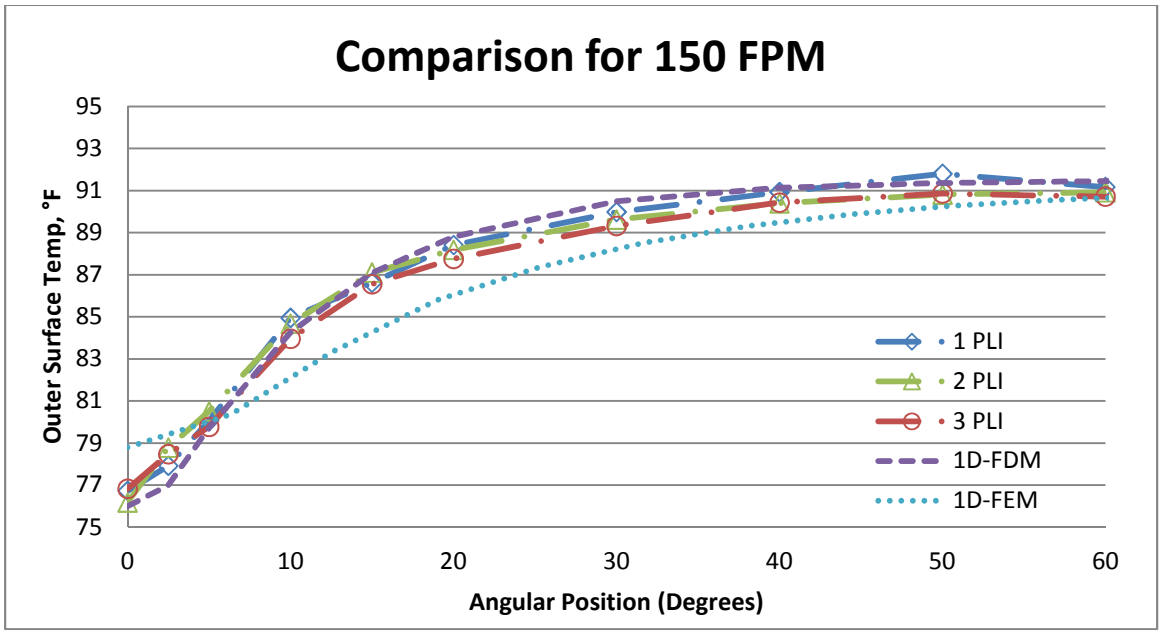

Figure 25 Comparison of FEA and FDM to Test Data, 150 FPM

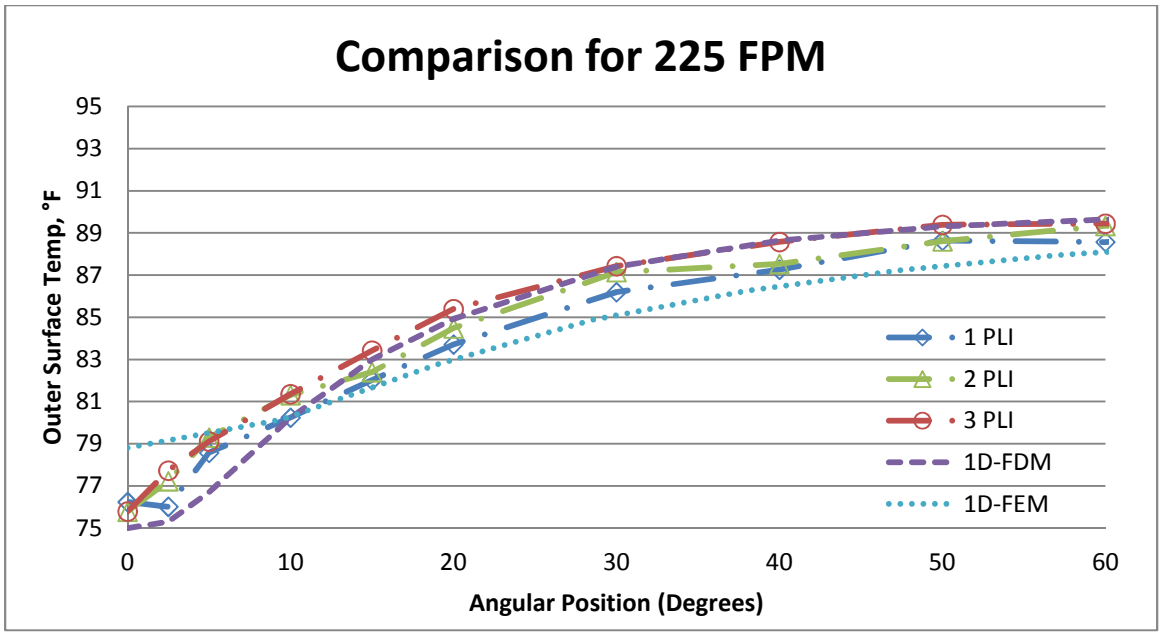

Figure 26 Comparison of FEA and FDM to Test Data, 225 FPM

It can be seen that, at most points, the FEM analysis is less than the value of the experimentally measure value. This may simply be due to the fact that only 16 time steps were use. The FDM method seems to predict the measurement data fairly closely even though perfect conduction was assumed and convection was neglected.

Next an analytical model was used based on solution of the heat equation determined by Pagilla and Lu[6]. This solution was implemented in MATLAB. This method was based on solving the heat equation by separation of variables, such that

$$\frac{\partial \theta}{\partial \tau} = \kappa \frac{\partial^2 \theta}{\partial y^2} \tag{4.7}$$

Where

$y - through\ thickness\ coordinate$

$\tau(x,t) - function\ of\ MD\ coordinate, x, and\ time\ , t$

Becomes

$$\frac{Y''}{Y} = \frac{T'}{\kappa T} \tag{4.8}$$

With the solutions

$$\begin{aligned} &T(\tau) = e^{-\lambda^2 \kappa \tau} \\ &Y(y) = Acos(\lambda y) + Bsin(\lambda y) \\ &\lambda - eigenvalues\ of\ the\ system \end{aligned} \tag{4.9}$$

By coupling the inner surface of the web and outer surface of the roller and applying the above equation to both, it could be determined that, for the roller

$$\begin{aligned} \vartheta_r(t, \tau_c) = \sum_{n=1}^{\infty} d_n [\tan(b\lambda_{rn}) \cos(y\lambda_{rn}) + \cos(y\lambda_{rn})\,] e^{-\lambda_n^2 \tau_c} \\ + \frac{\gamma(\theta_u - \theta_o)}{k_r + \gamma h \frac{k_r}{k_w} + b\gamma} (y + b) + \theta_o, -b \le y \le 0, \tau_c \ge 0 \end{aligned} \tag{4.10}$$

And for the web

$$\begin{aligned} \vartheta_w(t, \tau_c) = \sum_{n=1}^{\infty} d_n \frac{k_r}{k_w} \sqrt{\frac{\kappa_w}{\kappa_r}}\, [G(\lambda_n) \cos(y\lambda_{wn}) + \sin(y\lambda_{wn})\,] e^{-\lambda_n^2 \tau_c} \\ + \frac{k_r}{k_w} \frac{\gamma(\theta_u - \theta_o)}{k_r + \gamma h \frac{k_r}{k_w} + b\gamma} (y + b) + \theta_o, 0 \le y \le h, \tau_c \ge 0 \end{aligned} \tag{4.11}$$

The terms and definitions can be found in the original publication[6]. In the MATLAB code, the material thickness is divided into 1,000 points while the length of the contact area between the web and roller is divided into 220 points. At each point, for the time it takes a single point to transit the roll, the first 100 terms of the expressions above were summed to determine the temperature distribution through the thickness.

The values of the model plotted are the predicted surface temperature. For these models, the target value was set to the roller surface

temperature. This was done to better illustrate the differences between the expected values and the measure values.

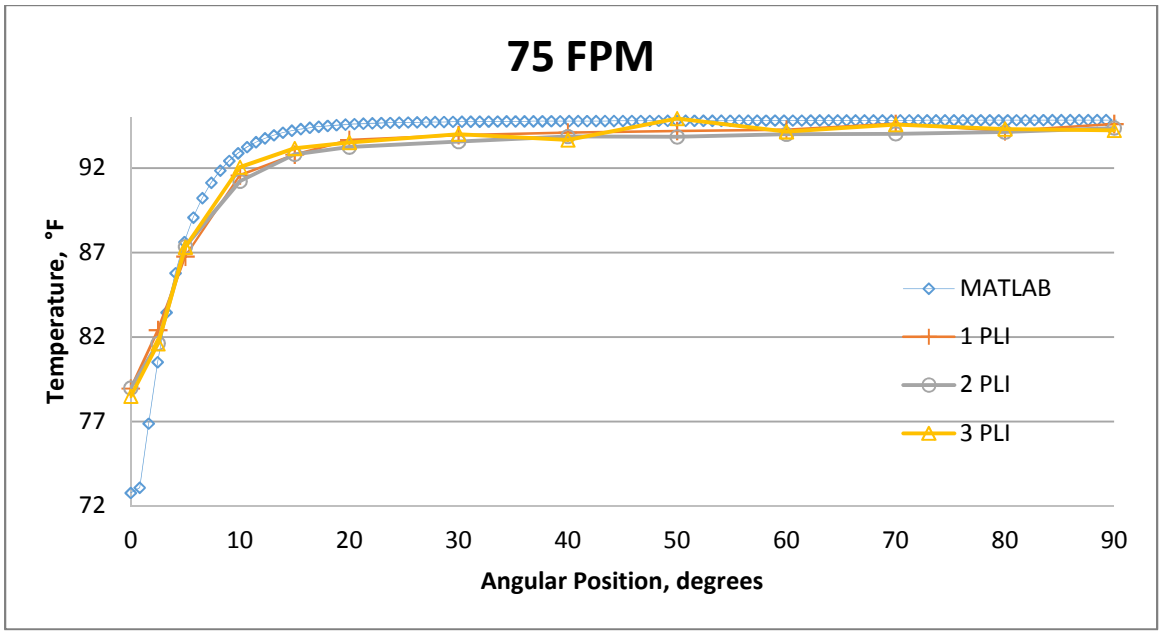

Figure 27 Comparison of Lu[6] curve to Test Data

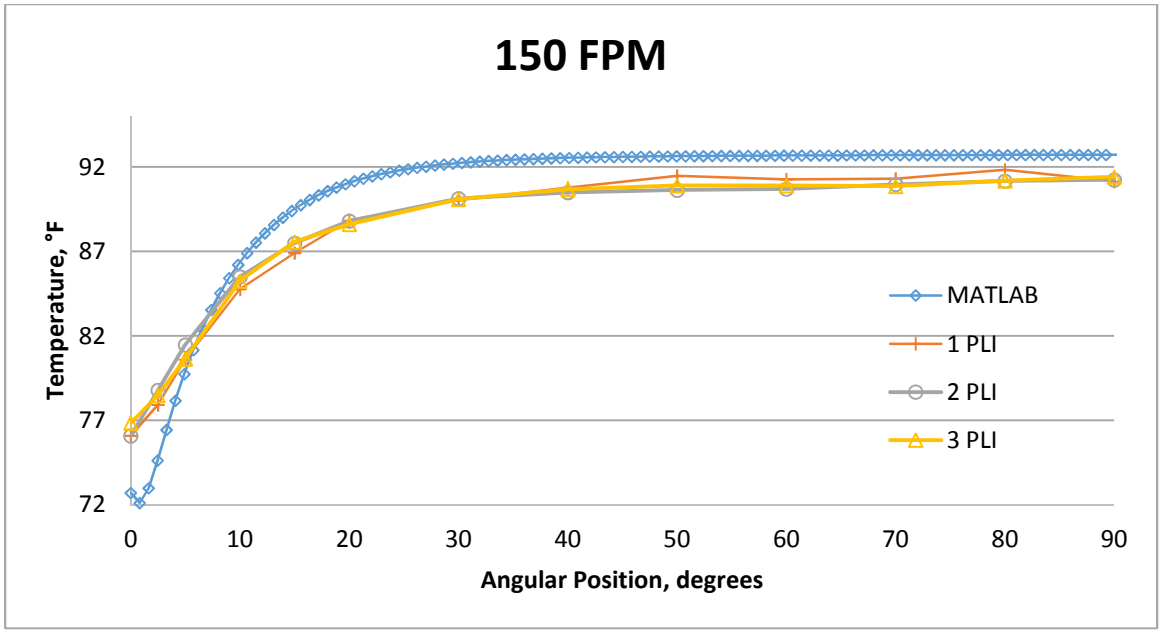

Figure 28 Comparison of Lu[6] curve to Test Data

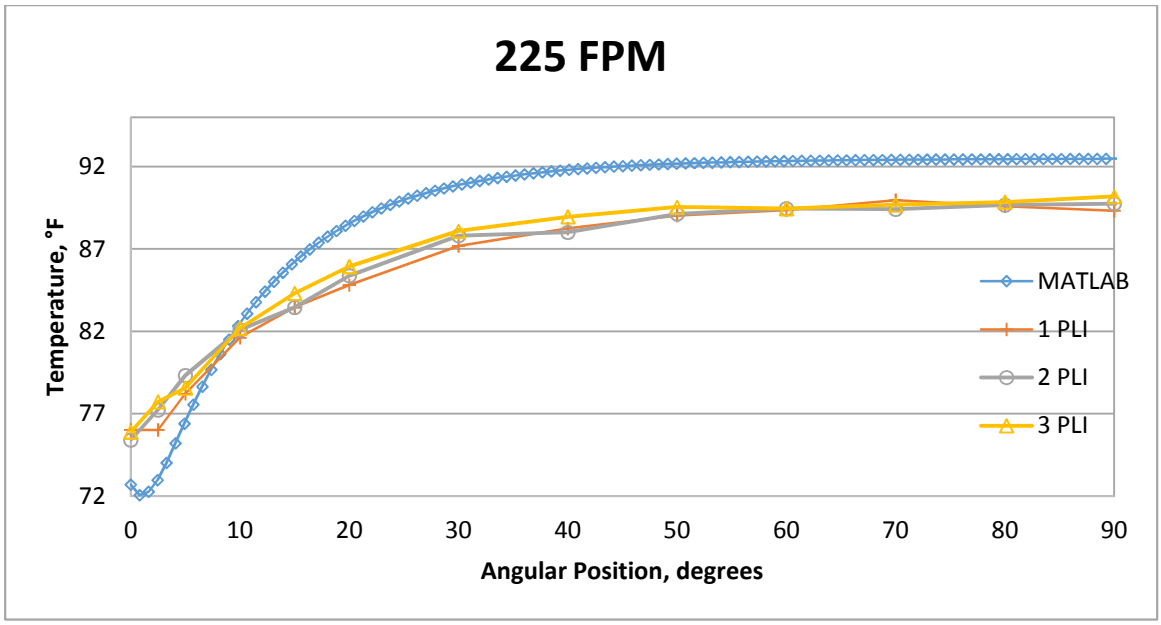

Figure 29 Comparison of Lu[6] curve to Test Data

Some of the observations from Chapter III can be seen in the preceding figures. In the plots in Chapter III it was observed that as line speed decreases, the initial measured value increases. This inversely proportional trend can be seen in the initial values of the plots on the previous page. As the line speed decreases, the difference in initial value between the Lu[6] solutions and experimental values increases.

It was also noted in the Chapter III plots that the effects of air entrainment seem to lower the asymptotic value reached in the web outer surface temperature as line speed increases. This effect is apparent in the plots on the previous page.

The use and comparison of these different analytical models has revealed that the experimentally obtained temperature curves behave like and can be predicted by analytical models, even if simple (FEM/FDM) models are used. However, for the analytical models to be accurate in predicting the

temperature on the roller, the temperature at entry and the asymptotic temperature value of the system must be known.

CHAPTER V

WRINKLING: EXPERIMENTAL SETUP & RESULTS

Since no wrinkling was observed during the temperature rise experiments, a different round of experiments was completed. The point of this set of experiments was simply to create wrinkles. During this set of experiments several observations were made about the behavior of the web as well. Since it is apparent from the equations in Chapter II that critical stress decreases as thickness decreases, the web used for these experiments was 92 gage (0.00092 inch thick) polyester, in lieu of the 200 gage.

The general procedure for this round of experiments was simply to increase the temperature of the roller, at a constant line speed and tension, until wrinkles appeared. In the initial experiment the temperature of the quenching oil medium in the heated roller was raised to its highest attainable value. However at the maximum achievable system temperature (approximately 160 °F) no wrinkles were observed. Therefore the system by which the roller temperature was controlled had to be changed so that higher temperatures could be achieved.

In lieu of the oil bath with a single submerged heating element, four 600 Watt heating elements, wired in parallel, were mounted on the roller's center shaft and suspended inside the heated roller. By running current

through these elements, the internal surface of the roller shell was heated by radiation. Voltage input to the heating elements was controlled manually via a Variac transformer. Applying ~100 Volts, the heating elements were able to achieve temperatures in excess of 800 °F, this allowed the external roller temperature to achieve temperature in excess of 500 °F.

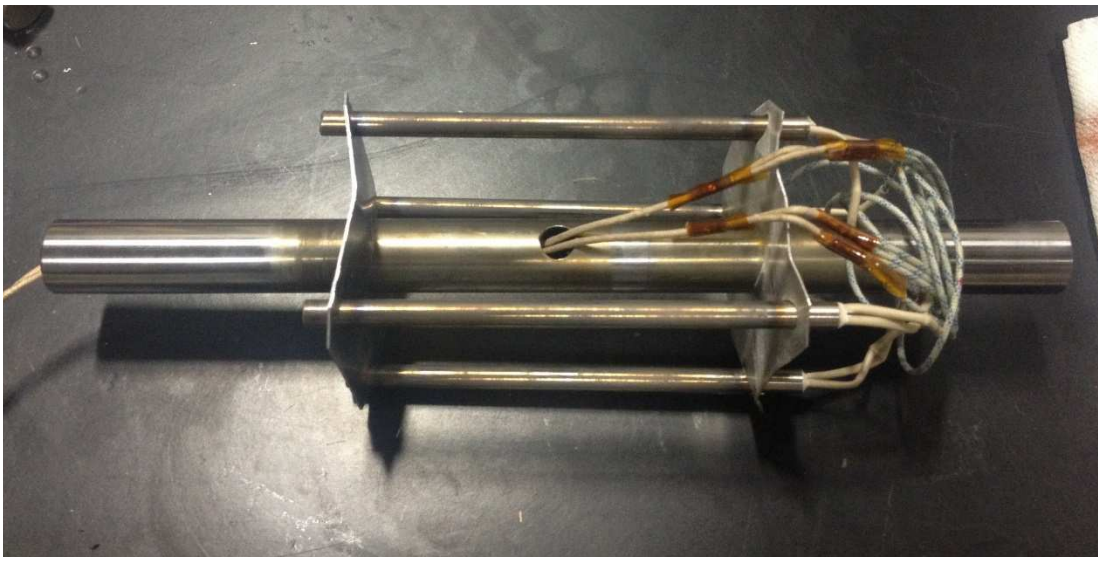

Figure 30 Radiation Heating Elements used in Wrinkling Test

To achieve wrinkling the web line speed and tension remained constant while temperature was increased. Line speed was set to ~30 FPM. This was done to minimize the effects of air entrainment and ensure the web reached the target temperature. Tension was set at 1.5 PLI. The initial temperature was set to 200 °F. Then the roller temperature was increased. Wrinkles were finally achieved due to temperature change at a roller surface temperature of ~300 °F.

During initial experimentation, wrinkling seemed to be sporadic, then it was observed that the web seemed more apt to wrinkle once it had been passed over the roller at 300 °F multiple times. It was also observed that the

width of the web seemed to decrease proportionally to the temperature increase as the web initially transited the heated roller. Static testing of samples of the web later revealed this to be the case. The details of web shrinkage test wills be outlined in Chapter VI. It was shown that when the polyester material was heated above its glass transition temperature (~150 ˚F) for the first time, the web dimensions would change. If the web was unstressed, and subjected to elevated temperatures the web dimensions would increase in the CMD and decrease in the MD. If web tension was applied, at elevated temperatures the web dimensions would decrease in the CMD and increase in the MD.

These observations lead to the realization that, upon initially being heated above glass transition temperature, the shrinkage of the web counteracted the thermal expansion of the web, decreasing the likelihood of wrinkling during initially being heated. This at least appears true in the case of webs which are oriented (stretched) during manufacturing. Therefore, in order to maintain repeatability and better observe wrinkling behavior the web material was heated to 300 ˚F under tension so that the material wouldn't shrink upon subsequent heating. Then the web was passed over the heated roller a second time to observe how web behavior and wrinkles varied with tension.

For this round of wrinkling test only one variable was changed. After the web had been heated once, line speed and temperature were maintained at ~30 FPM and ~300 ˚F. Then, tension was varied from 1 to 9 lbs (0.167 – 1.5 PLI) in 0.5 lbs increments.

At a tension of 9 lbs, no wrinkles were present. Wrinkles were not present at 8 lbs of tension either. Wrinkles began showing up sporadically at 6 lbs of tension. The following figures show conditions of wrinkling and not wrinkling for different tension values.

The figure below is for 9 lbs tension. At this tension level no wrinkles were observed.

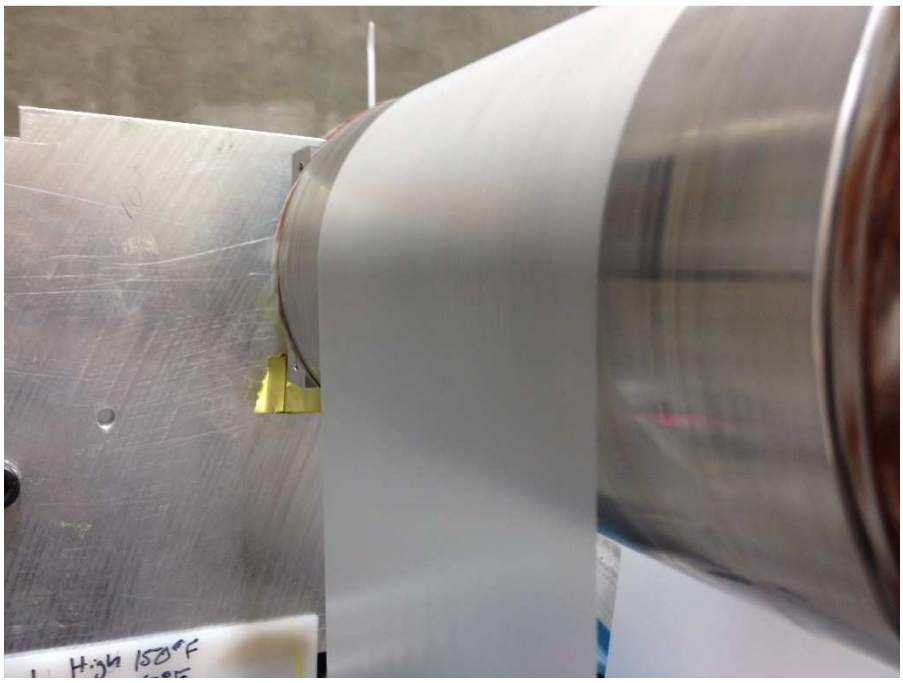

Figure 31 92 gage PET, 300 ˚F, 9 lbs tension

Wrinkles began appearing at 6 lbs of tension as seen in the figure below:

Figure 32 92 gage PET, 300 ˚F, 6 lbs tension

From 6 lbs down to 1 lbs of tension, wrinkles were present. The number and amplitude of the wrinkles increased as tension decreased.

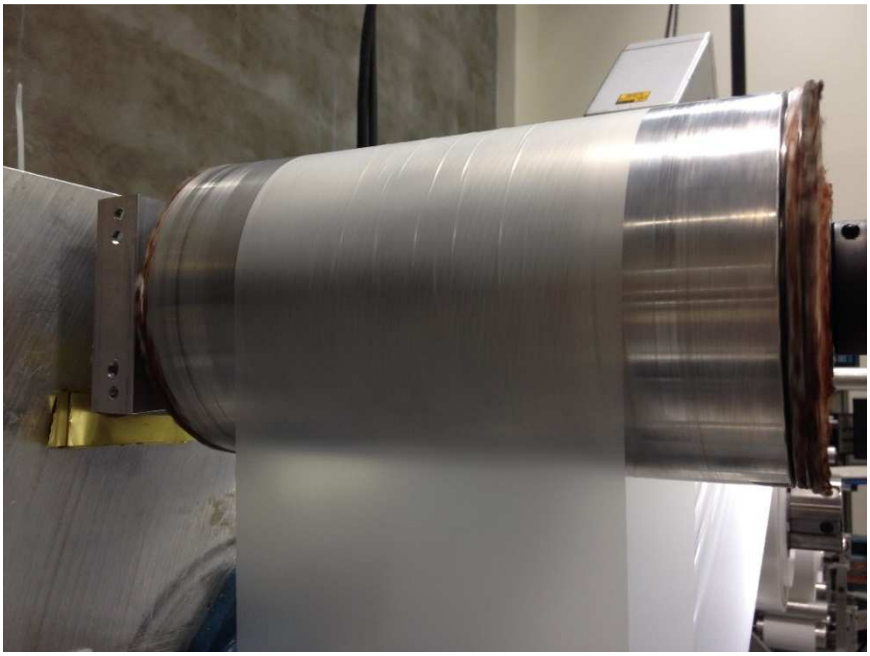

Figure 33 92 gage PET, 300 ˚F, 4.5 lbs tension

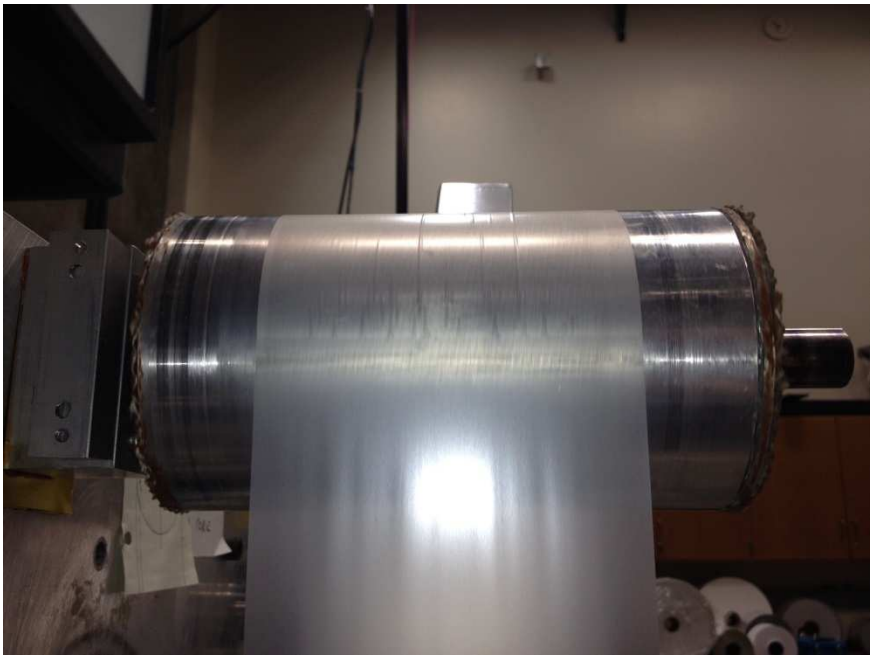

Figure 34 92 gage PET, 300 ˚F, 3 lbs tension

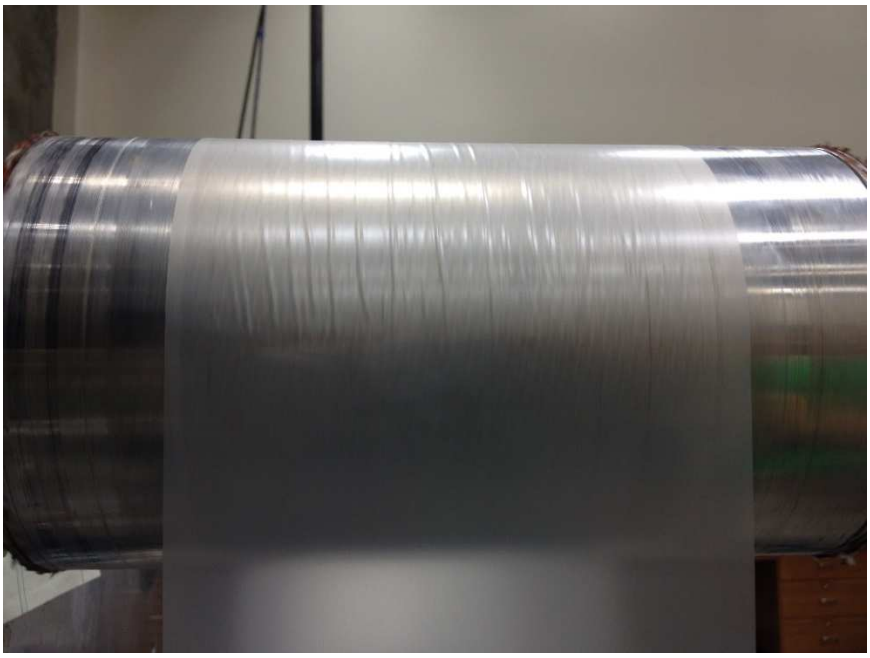

Figure 35 92 gage PET, 300 ˚F, 1.5 lbs tension

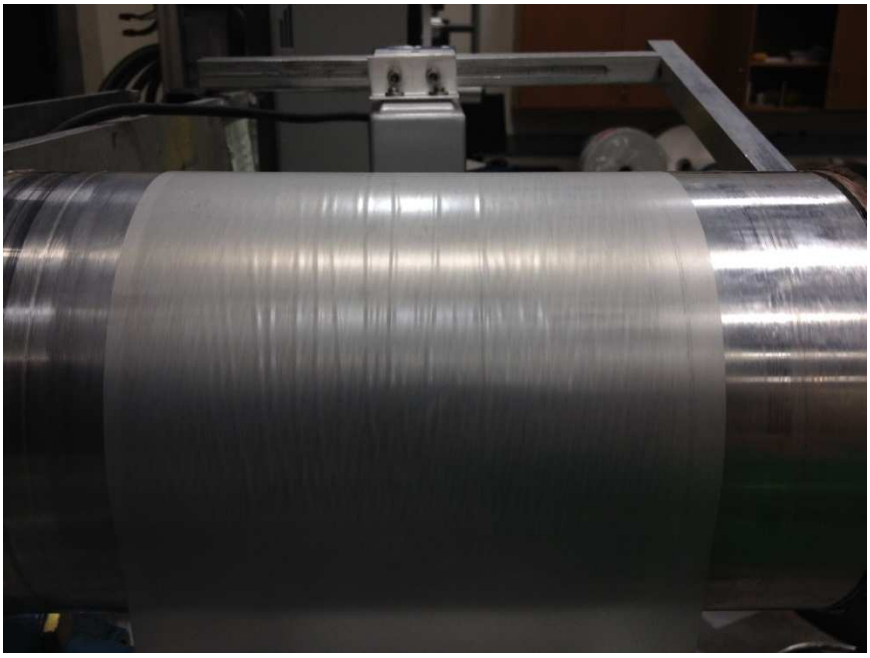

Figure 36 92 gage PET, 300 ˚F, 1 lbs tension

It was apparent from these experiments that probability of wrinkling is inversely related to line tension if line speed and temperature remain constant. The next step, after wrinkling is observed, is to use FEM to understand the state of stress during the conditions under which wrinkles do and do not exist.

CHAPTER VI

MATERIAL PROPERTIES TESTING

After the wrinkling experiments, the web was to be modeled using finite element analysis (FEA) in COSMOS/M. However in order for the FEA model to be accurate, the material properties of the web needed to be determined. The impact of the web transiting the heated roller on the room temperature material properties also needed to be determined.

The first test completed was a stretch test to determine modulus of elasticity. To do this, 50 foot long segments of polyester were stretched using a force gage. To complete the test, one end of the specimen was fixed and force was applied to the other end in 5 lbs increments from 0 – 25 lbs. Each time the force was increased, the displacement of the free end was marked so it could be measured later. 8 different test specimens were stretched from 2 different rolls of material. Three specimens were tested from the first roll. All three of these segments had been heated by transiting the heated roller. Five specimens were tested from the second roll of polyester. Of these five segments two had not been heated above the glass transition temperature, the remaining three specimens had been heated by transiting the heated roller.

After the stretch tests were completed, stress vs. strain curves were determined using the load-displacement data and the specimen geometry. The table below shows the load displacement data for all eight specimens. Force is measured in lbs, displacement is measure in inches.

Table 2 Force Displacement Data for Modulus Determination

F	dL1*^	dL2*^	dL3*^	dL4"	dL5"	dL6*"	dL7*"	dL8*"
00	0.000	0.000	0.000	0.000	0.000	0.000	0.000	0.000
05	0.760	0.765	0.810	0.711	0.670	0.525	0.505	0.695
10	1.550	1.475	1.475	1.365	1.310	1.240	1.220	1.390
15	2.285	2.215	2.225	1.980	1.965	1.955	1.945	2.040
20	3.035	2.995	3.020	2.715	2.715	2.680	2.645	2.755
25	3.805	3.765	3.805	3.360	3.300	3.395	3.405	3.490

* - Heated, ^ - Roll 1, " – Roll 2

For the data above, stress at each point was determine as

$$\sigma = \frac{P}{w * h}\ ,\ \ P - load, \qquad w - web\ width, \qquad h - web\ thickness \tag{6.1}$$

The strain at each point was determined as

$$\varepsilon = ln\left(\frac{L}{L_o}\right)\ , \qquad L - Total\ Length, \qquad L_o - Initial\ Length \tag{6.2}$$

The stress and strain values were then plotted and using the relation

$$\sigma = E * \varepsilon \tag{6.3}$$

the modulus of elasticity, E, was determined as the slope of a line plotted through the points.

The plot below is for Roll 1. It can be seen that for the specimens from Roll 1 the average value of Young's Modulus is 721.5 ksi. The value reported by the manufacturer, in the MD, is 710 ksi. So the modulus seemed relatively unchanged by transiting the heated roller.

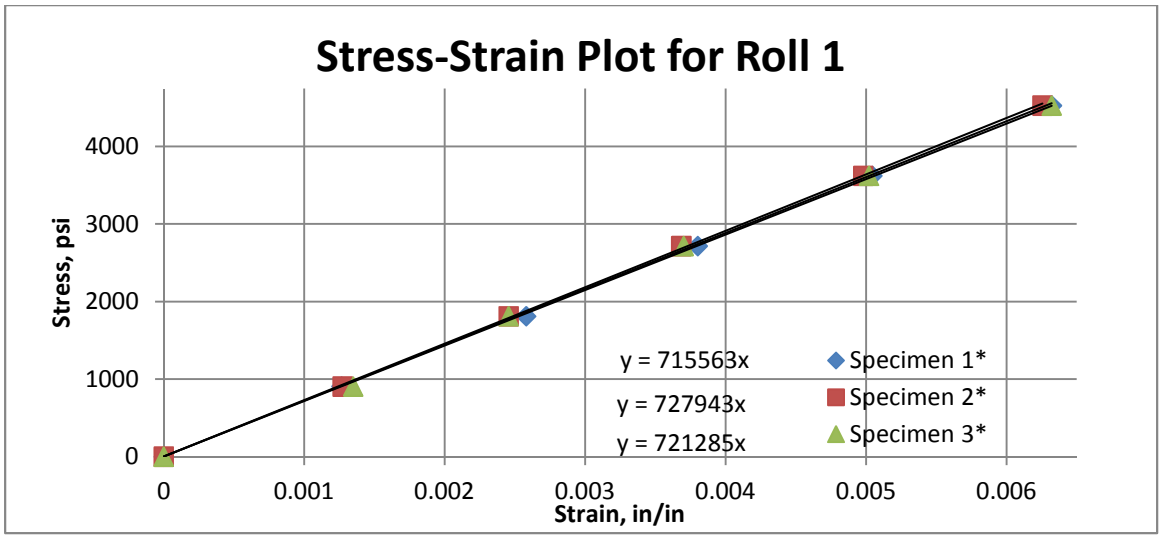

Figure 37 Stress-Strain Data for Roll 1 Modulus

The plot below is for Roll 2. It can be seen that for the heated specimens from Roll 2 the average value of Young's Modulus is 806.7 ksi. While, for the unheated specimens from Roll 2, the average value of Young's Modulus is 810.8 ksi. Therefore while there is a difference between the rolls, the effect of heated and cooling does not seem to permanently affect the modulus of the polyester.

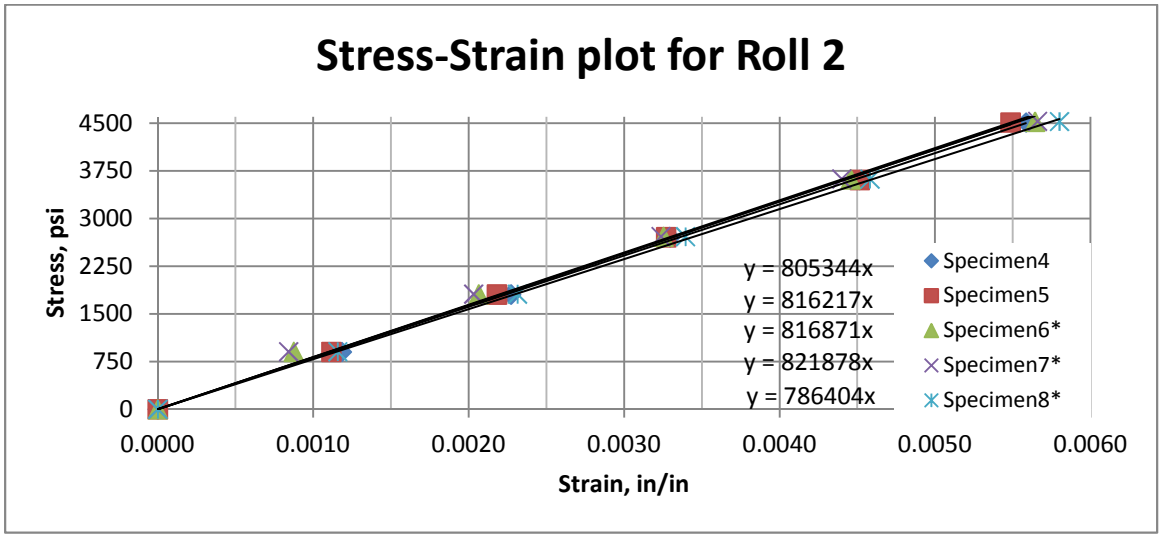

Figure 38 Stress-Strain Data for Roll 2 Modulus

Since the roll with the modulus of ~800 ksi is the one used for the majority of the wrinkling experiments, this is the value used in the FEA model. It was observed, however, in literature from DuPont that the modulus of the polyester does decrease logarithmically as a function of temperature[10].

As stated in the previous chapter, it was observed that the material seemed to shrink in the CMD as a function of temperature and tension. A series of experiments was completed to determine how dimensions of the web changed in different conditions. First, 6 inch squares of polyester were placed into an environmental chamber and heated, unstressed, to a temperature of 300 °F. This was done in compliance with ASTM D1204[12]. Specimens were allowed to soak for 30 minutes. Afterward measurements were then taken to determine changes in MD and CMD directions. Secondly, polyester pieces were placed into the environmental chamber and a 1.5 PLI static tension force was applied. These pieces were also heated to 300 °F and allowed to soak for 30 minutes. These pieces were measured in the same manner as the first. Lastly, measurements were taken of web sections immediately upstream and downstream of the heated roller. The roller was heated to 300 °F, and line speed was set to 30 FPM. Tension values were varied between 1.0 - 2.0 PLI. In the last case, only CMD values were measured. The average values for shrinkage in each case are shown below.

Table 3 Shrinkage due to Temperature and Tension

Method of Heating	Tension Value	Average %change, MD	Average %change, CMD
Environmental Chamber	0.0 PLI	-1.126	0.323
Environmental Chamber	1.5 PLI	1.166	-0.831
Transit Heated Roller	1.0 PLI	N/A	-0.208
Transit Heated Roller	1.5 PLI	N/A	-0.498
Transit Heated Roller	2.0 PLI	N/A	-1.037

From the table above it can be seen that as tension in increases, the web elongates in the MD and contracts in the CMD. It can also be seen that the contraction in the CMD is different for the values of 1.5 PLI between the specimens heated in the environmental chamber and those heated by transiting the roller. The contraction of the material which transited the roller is roughly 60% of that which was allowed to soak in the chamber. At a rate of 30 FPM, the web is in contact with the roller for approximately 1.44 seconds. This means that the majority of the contraction which takes place due to the elevated temperature happens fairly quickly.

As stated earlier this contraction also provides a possible explanation as to why the web does not wrinkle the first time it transits the heated roller. The contraction of the web counteracts the effects of thermal expansion. If it contracts enough to keep the edge of the material from slipping then wrinkles will not occur.

The next set of property experiments was completed to determine the thermal coefficient of expansion of the material. To do this, 10 inch long specimens were hung from an aluminum frame inside the environmental chamber. Then a rod was run from the free end of the specimen, out of the chamber and connected to a linear variable differential transformer (LVDT)

mounted vertically outside of the chamber. This allowed any change in length to be recorded to a fairly high degree of precision.

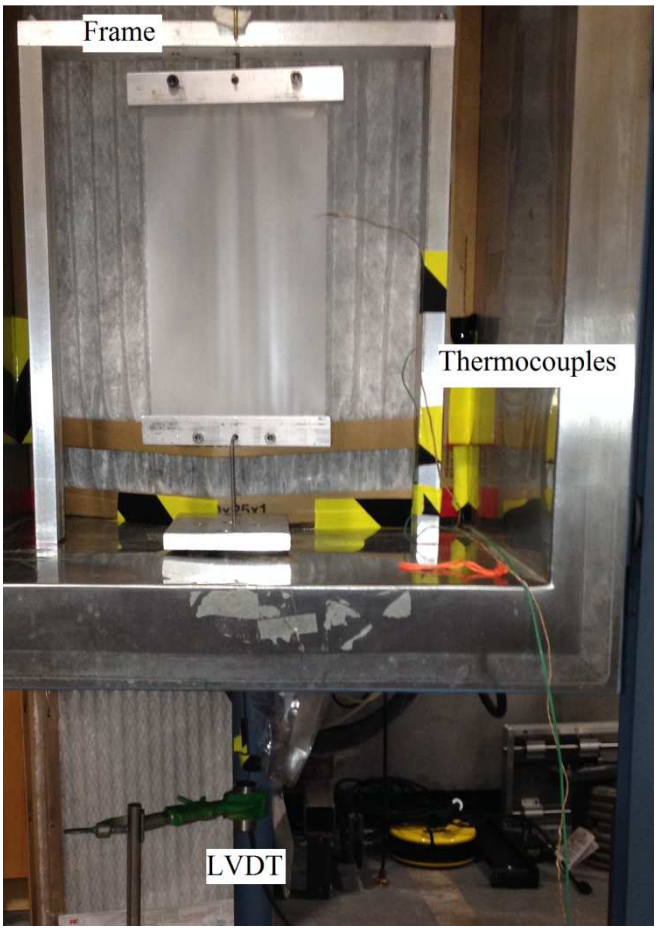

Figure 39 CTE Test Stand and Sensors

The specimens were heated from 90 – 150 °F. During the heating process, the temperature of the material and frame were recorded with thermocouples while as the position of the sensor data was recorded using LabView. Three types of specimens were tested: (1) specimens that had not been heated above room temperature, (2) specimens that had been heated by transiting the heated roller, (3) specimens that had been heated in the environmental chamber and allowed to soak at 300 °F.

Four specimens of each type were used. For each test, a temperature vs. strain curve was created. The coefficient of thermal expansion (CTE) was taken as the slope of the curve (in/in/°F). The recorded displacement for each specimen was converted to strain by accounting for the vertical expansion of the frame and dividing by the specimen length. For 3 specimens, data was recorded during heating. For the 4th specimen, the data was recording for both heating and cooling. The CTE of each specimen is shown below.

Table 4 Test CTE Values

Specimen	Type	CTE (in/in/°F)
1	1	0.000032
2	1	0.000028
3	1	0.000027
4	2	0.000021
5	2	0.000026
6	2	0.000023
7	3	0.000033
8	3	0.000036
9	3	0.000037
10	1	0.000026
10	1	0.000020
11	2	0.000030
11	2	0.000016
12	3	0.000029
12	3	0.000016

From the adjacent table it can be seen that the CTE ranged from 15 – 37 µinches/inch/°F. The CTE did not appear to fluctuate proportionally with temperature or method of heat treatment. Therefore, for the modeling portion of this research, a value of 25 µinches/inch/°F was used.

The last property to be determined was the coefficient of friction between the polyester and the heated roller. To do this, the band brake equation was utilized: The band brake equation is utilized to show the relationship between a belt and a rotating cylinder. The tension force in the belt, the friction coefficient between the belt and the cylinder, and the wrap angle are related by:

$$\frac{T_1}{T_2} = e^{\mu\theta} \quad or\ \mu = \frac{1}{\theta}\ln\frac{T_1}{T_2} \tag{6.4}$$

where,

$T_1 - Tension\ in\ direction\ opposing\ motion,$
$T_2 - Tension\ in\ direction\ of\ motion,$
$\mu - coefficient\ of\ friction,$
$\theta - wrap\ angle\ (radians)$

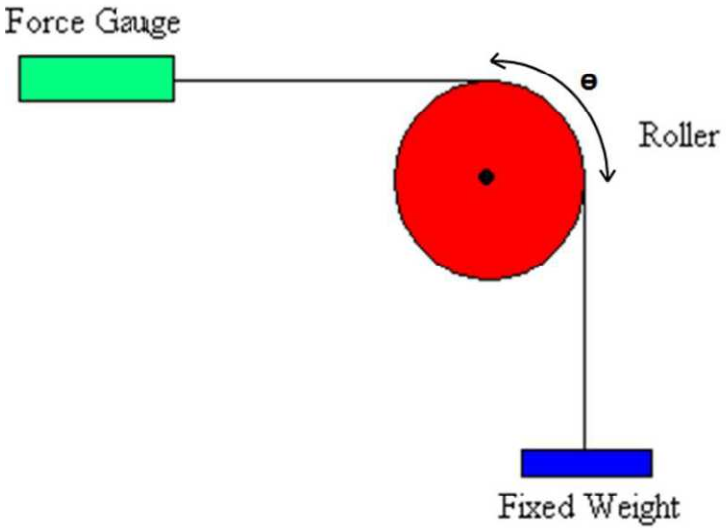

Figure 40 Band Break Test Configuration

To determine μ a piece of web was dragged across the heated roller at room temperature. The roller was held stationary. On one end of the material a weight was attached (9 lbs), on the other end a force gage was hooked onto the material. A wrap angle of 90 degrees ($\pi/2$ radians) was used. The material was pulled across the roller in one direction and then allowed to slip in the other. Under each the condition the force gauge output was recorded. The results are as follows:

Table 5 Coefficient of Friction

	T2 (lbs)	T1 (lbs)	θ	μ
Pull	9	~12.5	1.570796	~0.209
Slip	~6.5	9	1.570796	~0.207

From the data shown it can be seen that the coefficient of friction is about 0.21. Therefore, a value of 0.21 was used in the analytical model.

The value of Poisson ratio was taken from the manufacturer's data. From the manufacturer value was given as 0.38. This value was used for all temperatures. With the material properties determined, a FEA model could be assembled.

CHAPTER VII

MODELING

After the completion of the wrinkling and material property experiments, an FEA model was created to simulate the conditions under which wrinkling occurred. The model included the upstream span and downstream span in addition to the area in contact with the heated roller. The figure below is representative of the model that was used. The figure also shows the boundary conditions that were applied as well.

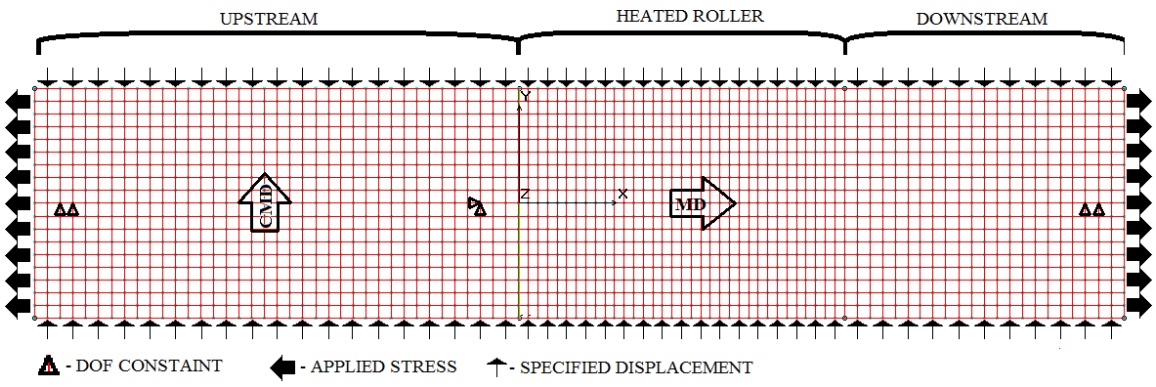

Figure 41 COSMOS/M Model

The model is 6 inches wide. The upstream section is 22 inches long. The contact section is 8.5 inches long. The downstream section is 10 inches long. Several nodes along the centerline of the model (Y=0) were constrained in the Y-direction to create symmetry about the centerline. One node on the

model centerline was constrained in the x-direction to provide stability. Each section of the model utilized quadrilateral shell elements. The model was divided into 18 elements in the CMD. The upstream and downstream sections contained 3 elements/inch in the MD while the contact section contained 4 elements/inch in the MD.

The simulation was a run as a nonlinear static analysis. The analysis was run over a 10 unit interval at 0.5 step increments. There were 3 boundary/loading applied to the model over the 10 unit interval:

1. The first load created an applied stress in the MD. This was done to induce the stress the web would undergo in the free span before heating. The value of the applied stress at a given increment was equal to the applied line tension (PLI) multiplied by the stress time curve value divided by the material thickness (0.00092 inches). The time curve for the applied stress is shown in the following figure.

$$\sigma(t) = \frac{C_1(t) * T}{h} \tag{7.1}$$

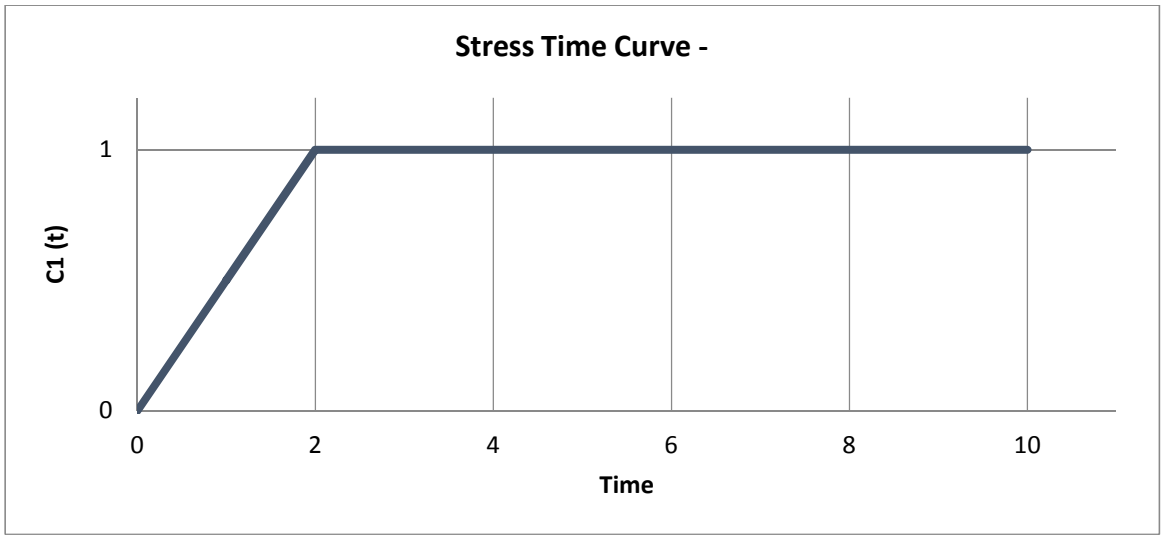

Figure 42 FEM Time Curve for Stress

2. The second loading condition was a specified displacement of the edges of the web. Each edge was displaced toward the material center. The displacement was equal to the value of the Poisson contraction that the web would undergo before heating. Enforcing and maintaining this displacement creates a condition of normal (perpendicular) entry of the web to the heated roller. This normal entry condition also represented a condition in which the web was unable to slip on the roller due to friction. The value of the Poisson contraction and applicable time curve is shown in the following figure.

$$U_y(t) = \frac{C_2(t) * T * \nu * w}{2 * h * E} \tag{7.2}$$

Where

$T - Line\ Tension$
$\nu - Poisson\ ratio$
$w - width\ of\ web$
$h - thickness$
$E - Young's\ Modulus\ at\ room\ temperature$

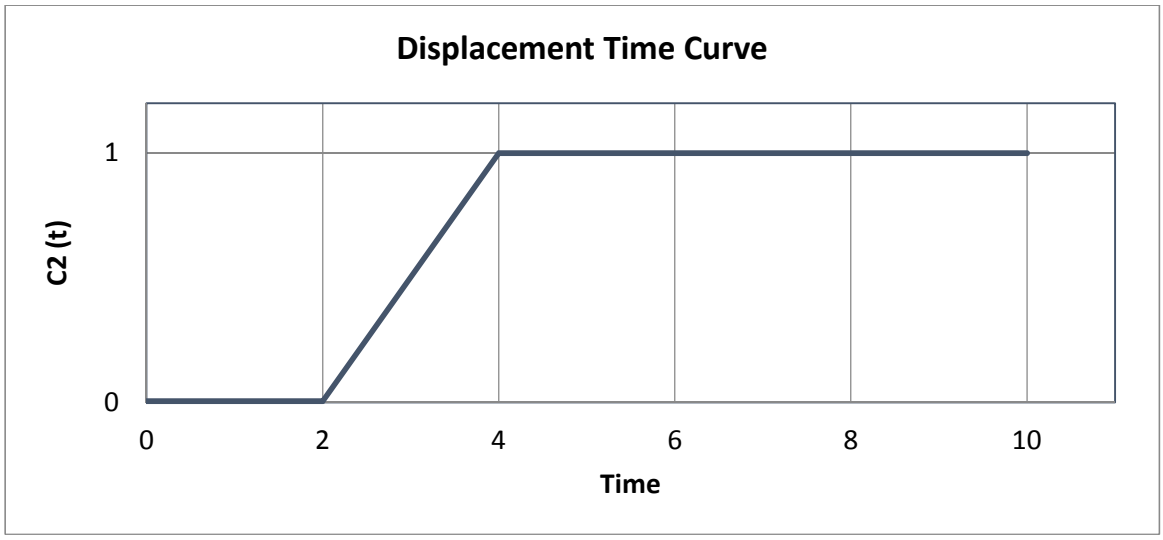

Figure 43 Time Curve for Displacement

3. The third loading was for the applied change in temperature at each node. The change in temperature was specified at each node. The temperature was maintained in the CMD at any given MD location. In the upstream section there was no change in temperature. In the downstream section the change in temperature decreased linearly. In the contact section, a temperature curve was created based on readings and observations taken during the wrinkling experiments. The change in temperature ranged from 0 – 228 ˚F based on the difference between the room temperature (72 ˚F) and the roller temperature (300 ˚F). The temperature curve and the applicable time curve are shown below.

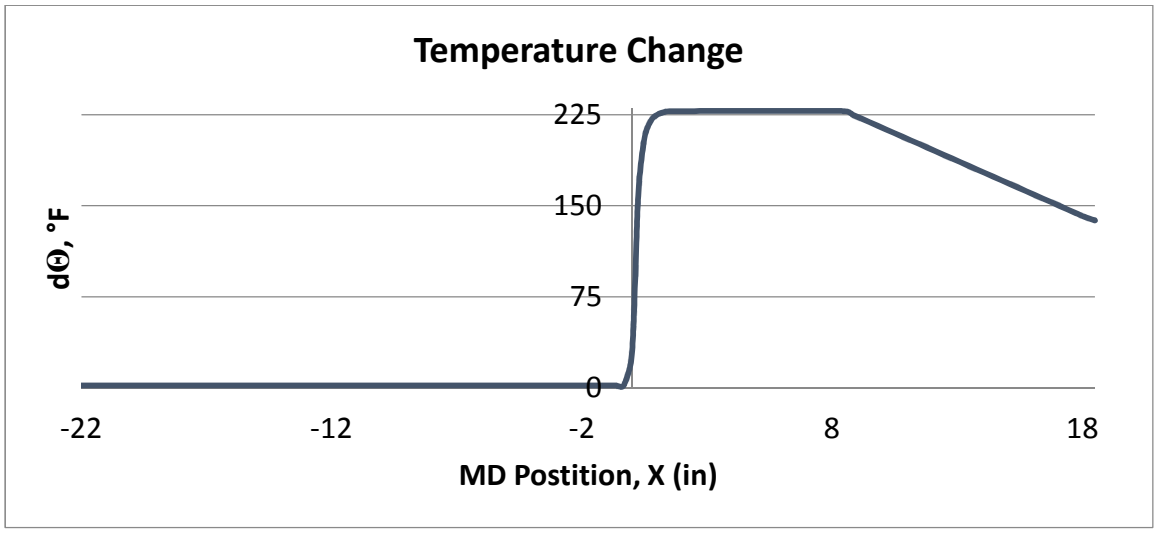

Figure 44 COSMOS/M Temperature Profile

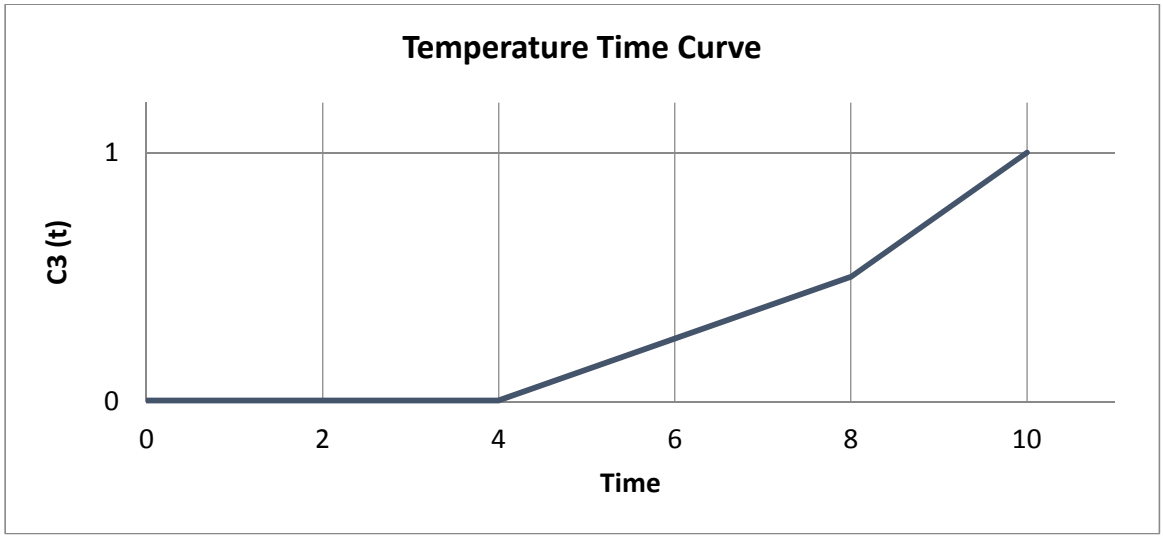

Figure 45 Time Curve for Temperature

The temperature increase at any given time and position is given by

$$\Delta\Theta(x,t) = C_3(t) * d\Theta(x) \tag{7.3}$$

A temperature dependent material property curve was also created for the model. In a previous section it was stated that the Young's Modulus of the material was ~800 ksi at room temperature. However, according to the

manufacturer's data, the modulus of the material decreases as temperature increases[10].

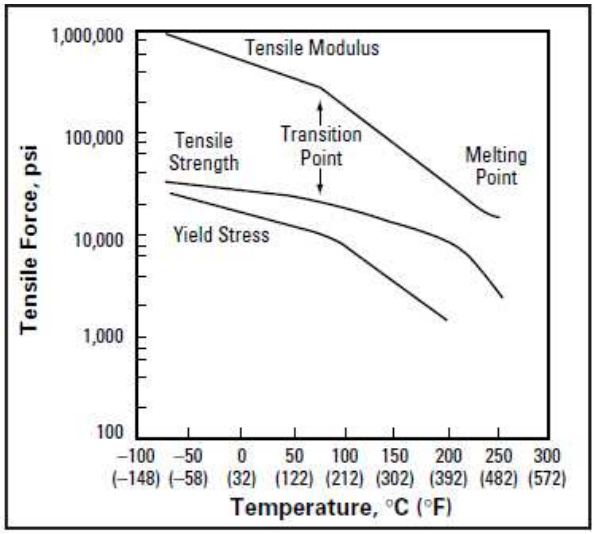

Figure 46 Manufacturer's Modulus Curve

So in order to compensate for this decrease, a correction factor was applied to the manufacturer's values. The correction factor was based on the ratio of the determined modulus and the values form the chart above at 72 °F. A correction value of ~1.86 was used to create a temperature curve to be used in the model as follows.

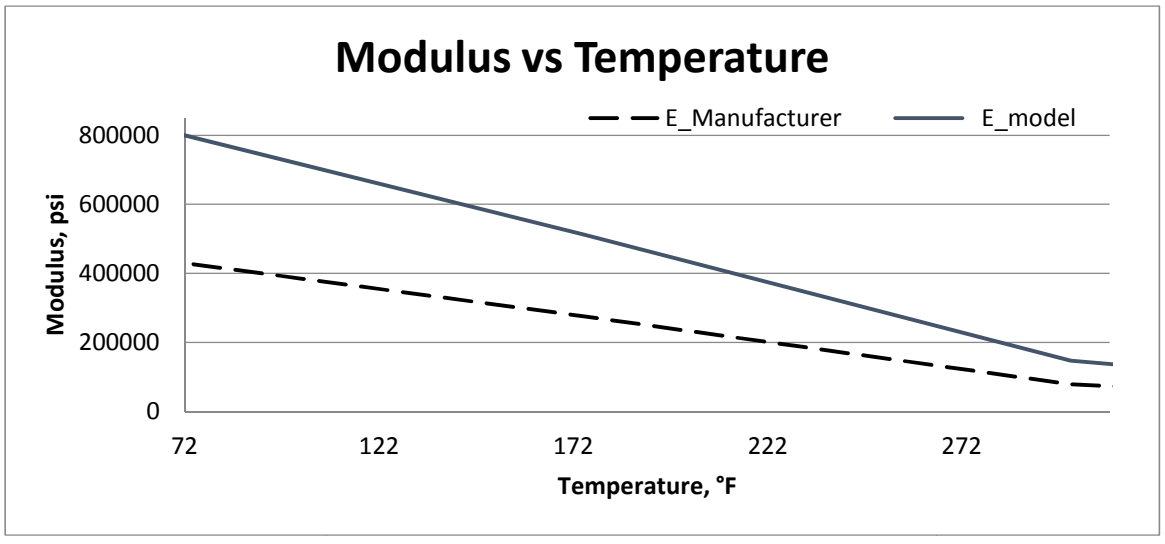

Figure 47 Temperature Dependent Modulus Curve

From the wrinkling experiments it was determined that wrinkles were present below tension levels of 1.0 PLI. Therefore, simulations were run for

3 different tension values: of 0.25 PLI and 2.0 PLI as well as a value to be determined later. After these simulations were run the mean value of the CMD stress along the center line of the contact area was recorded. These values were then compared to both the maximum stress value sustainable by friction between the web and roller as well as the Timoshenko critical buckling stress.

For a web-roller interface, the contact pressure between the web and roller is given as:

$$P_c = \frac{T}{R} \tag{7.4}$$

where

$R - radius\ of\ roller$

$T - Line\ Tension$

which means that the maximum force due to friction per unit circumference that can be achieved along the web centerline is

$$F_{fr} = \mu * \frac{w}{2} * P_c * 1 \tag{7.5}$$

Where

$\mu - coefficient\ of\ friction$

$w - width\ of\ web\ in\ CMD$

Therefore the maximum stress value sustainable by friction is:

$$\sigma_{fr} = \frac{F_{fr}}{h * 1} \tag{7.6}$$

where

$h - web\ thickness$

As mentioned earlier, the Timoshenko buckling stress is

$$\sigma_{cr} = \frac{-E * t}{\sqrt{3 * (1 - \nu^2)} * R} \tag{7.7}$$

To be conservative, the room temperature value of E was used in the initial determination of σ_{cr}.This led to a critical stress value of 167 psi.

The results of the 0.25 PLI simulation are shown below. It should be noted that for this case, the applied stress value was 271 psi. The edge displacements were ±0.00038 inches. As a result the average value of the compressive stress along the material centerline due to thermal expansion is -780 psi.

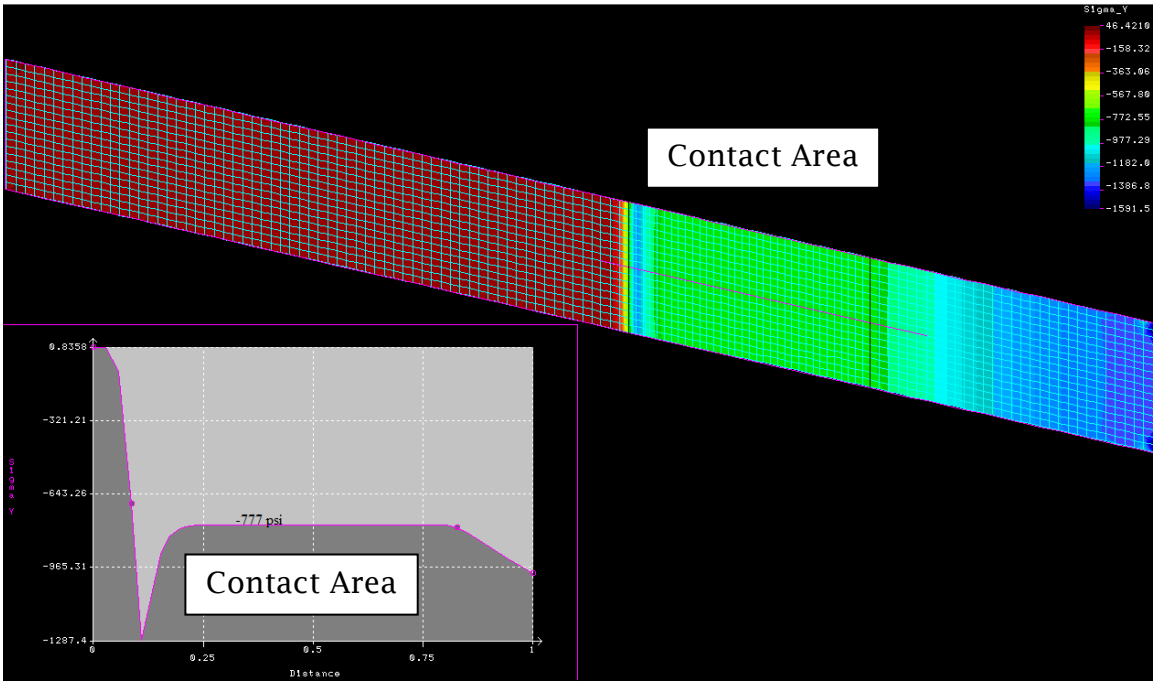

Figure 48 0.25 PLI, Sigma-Y Stress plot

The maximum sustainable stress, σ_{fr}, is -171 psi. Since the centerline stress value is greater than the sustainable stress value, slippage will occur outwardly on the roller. At steady state, it is the tendency of the web to come onto the roller at right angles to the roller axis [16]. This slippage will

create outward (negative) steering of the material edges. The following figures illustrate both normal entry and negative steering angles. Since the web will seek to attain normal entry, the edges will steer inward which will gather material in the center of the web. Since both the generated and sustainable stress values are above the critical buckling stress, the gathered material is expected to generate wrinkles. This is in agreement with the results found during the wrinkling experiments.

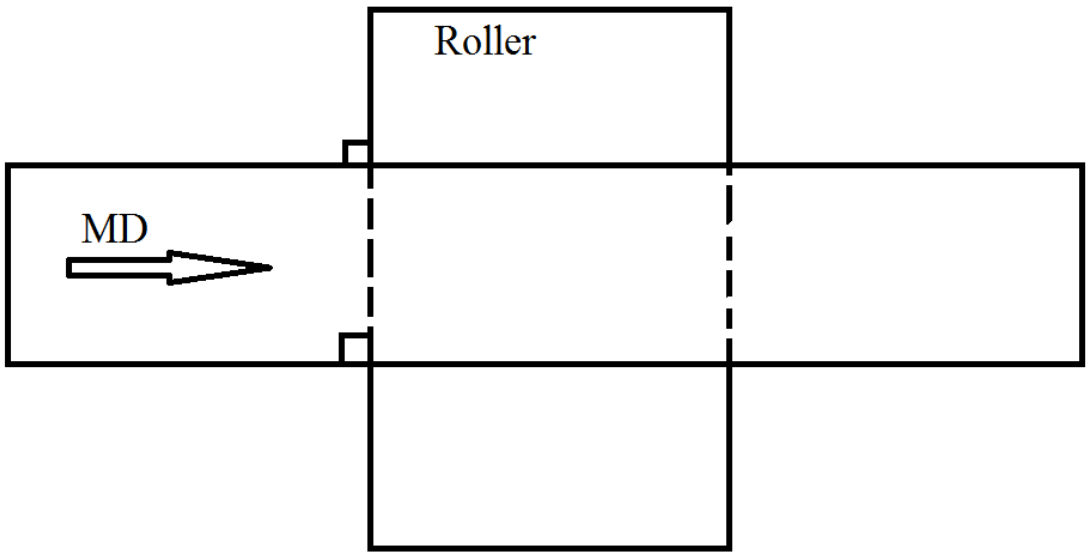

Figure 49 Normal Entry of web onto roller

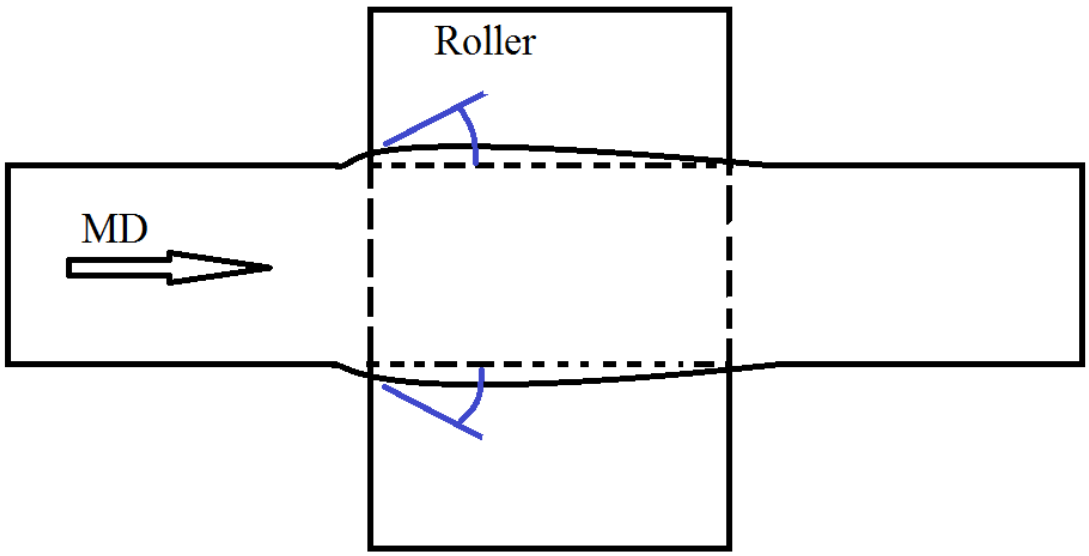

Figure 50 Web with negative steering angles at entry

The result of the 2.0 PLI simulation is shown below. It should be noted that for this case, the applied stress value was 2174 psi. The edge displacements were ±0.0031 inches. As a result the average value of the compressive stress along the material centerline due to thermal expansion is -193 psi.

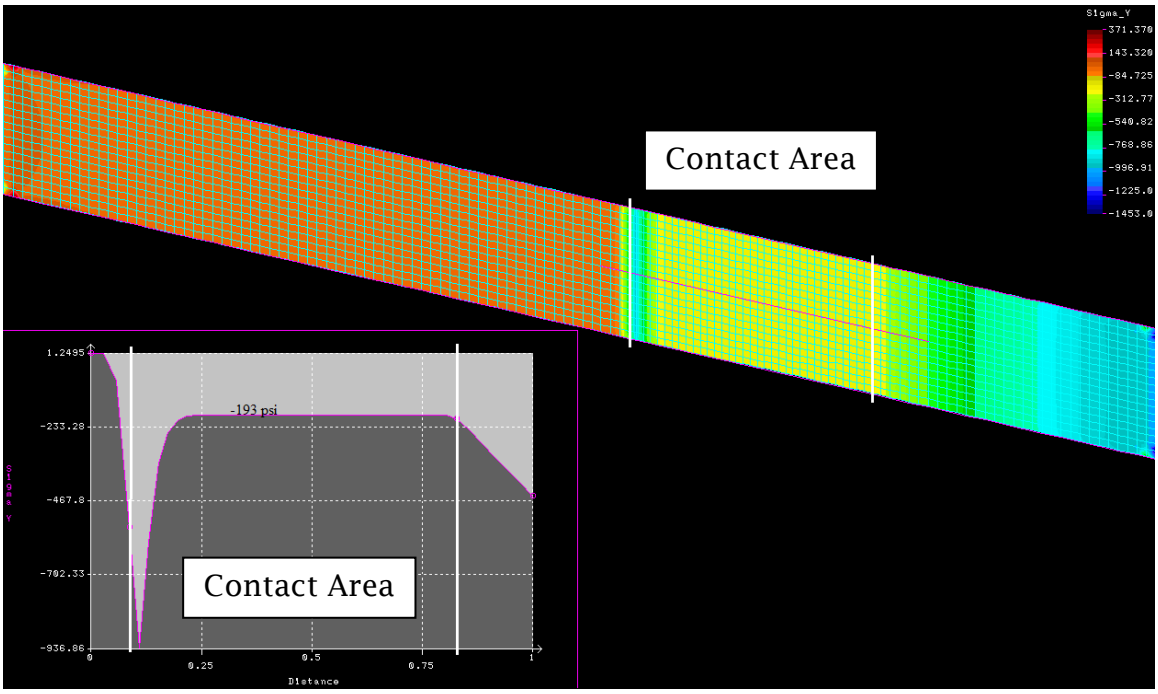

Figure 51 2.0 PLI, Sigma-Y Stress plot

The maximum sustainable stress, σ_{fr},is -1368 psi. Since the centerline stress value is much less than the sustainable stress value, slippage is not expected to occur. This lack of slippage will not create steering of the material edges because the frictional force will maintain normal entry. Therefore even though both the generated and sustainable stress values are above the critical buckling stress there will be no gathered material and no wrinkles will be expected to generate. This is also in agreement with the results found during the wrinkling experiments.

Since it was determined that slippage will would occur in the model at 0.25 PLI, but not at 2.0 PLI the next step was to find the point where the generated stress and sustainable stress are equal. During the lab experiments, it was found that wrinkles started to sporadically form and dissipate at a tension of 1.0 PLI. Therefore, 1.0 PLI was a starting point,

however in the model slippage wound not occur. It was found, in the model, that at 0.85 PLI, sustainable and generated stresses were both ~-580 psi.

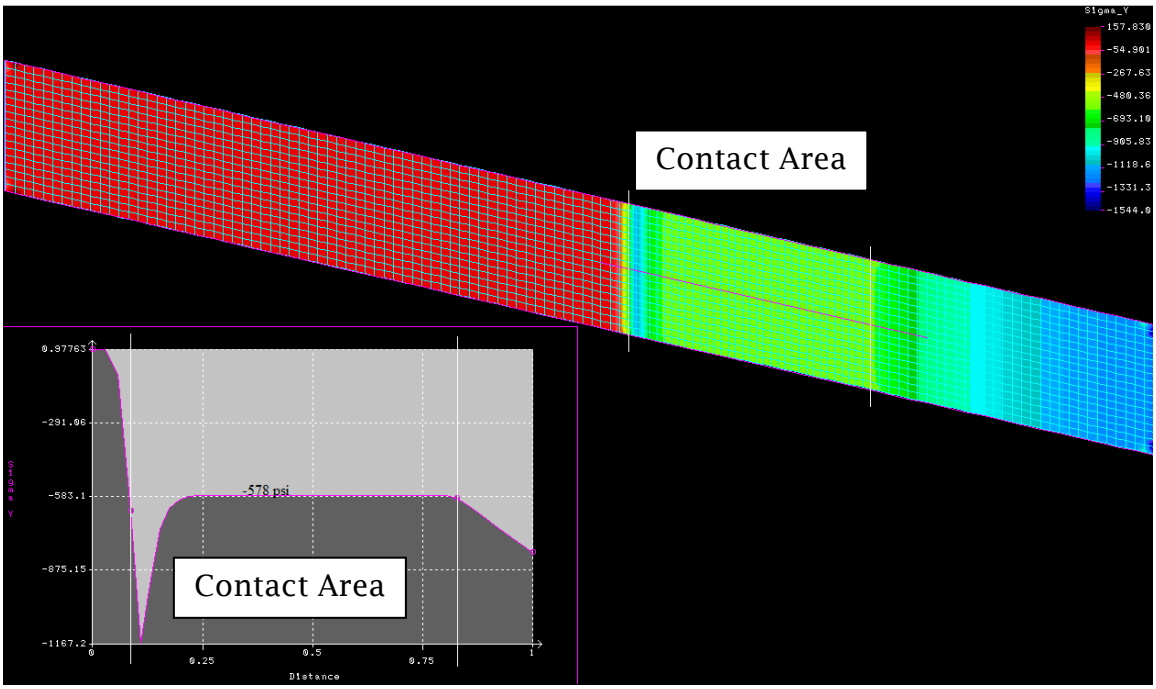

Figure 52 0.85 PLI, Sigma-Y Stress plot

So at this value of 0.85 PLI, in the model, wrinkling is on the verge of occurring if tension is decreased, or not occurring at all if tension is increased. This would be similar to the behavior seen at 1.0 PLI during the wrinkling experiments.

Overall the model and experiments seem to be in agreement. However, the discrepancy between 1.0 PLI value seen in the lab and 0.85 PLI seen in the model may be corrected if a full modulus vs temperature curve had been acquired or if friction in the model had been applied directly in the model.

It can also be seen in the figures above that there exist a discontinuity point in in the stress plot, just after the contact area begins. This

discontinuity appears to be a product of the temperature-dependent modulus. In the start contact area the temperature gradient is quite large (130 ˚F/0.25 inch), it was seen that if the modulus was keep constant with temperature no discontinuity was generated. However the model and the experimental data were largely different in that case. Therefore the modulus had to be allowed to change, but it appeared that the combination of the high temperature gradient and large drop in modulus caused some extrapolation/interpolation errors in the model. Nonetheless since the model seemed well behaved in the majority of the contact are this discontinuity was not seen as enough of an error to invalidate the model.

LIMITATIONS

It should be noted that there are some limiting factors in this model that need to be considered. The first of which is that lack of friction within the model. In reality, friction affects stress and displacement in both the MD as well as the CMD. In both directions, there will be areas which slip and areas which do not. In areas which do not slip, thermal expansion would cause reduction in the MD stress and strain and compressive stress in the CMD. In areas of slippage, there would be gradients in both stress and strain. This is not reflected in the model. The effect of friction is disregarded in the MD. Also the effects of slippage are disregarded in both MD and CMD. This means that the model is accurate in the CMD until the point that slippage occurs. This does not discredit the model, however, in the scope of this research, since the point at which slippage occurs is used as the criterion for wrinkling of the web.

CHAPTER VIII

CONCLUSIONS

Experiments were conducted in this research to try and observe the behavior of polyester webs transiting a heated roller. Also analytical and FEM models were created to compare the experimental results to. As a result the following conclusions can be drawn from this research:

1. Though the inner surface of a web transiting a heated roller is assumed to instantaneous achieve the temperature of the roller, as Chapters III shows, it does take time for the web to achieve uniform temperature through its' thickness even if the thermal mass of the roller is much greater than the web.
2. If the entry temperature and asymptotic exit temperature of a web transiting a heated roller are known, then the web temperature profile on the roller can be predicted using a number of different heat transfer models. As the results of Chapter IV show, FEM, FDM and differential equation solutions are effective. However, radiation and convection acting on the entry span and air entrainment between the web and roller must be accounted in the model to to predict an accurate temperature rise over the contact arc.

3. If a web is oriented, when it is heated above its glass transition temperature for the first time by transiting a heated roller under tension, it will undergo shrinkage in the CMD. This shrinkage will decrease the likelihood of the web wrinkling since it counter acts the effects of thermal expansion. These shrinkage effects will diminish after the first times the web is heated.
4. If a web is heated to high temperature at a relatively low tension, then wrinkling will occur. If tension is decreased while all other variables remain constant, the number and amplitude of the wrinkles will increase.
5. Heating a polyester web above its glass transition temperature does not affect its elastic modulus once the material is cooled again. However the modulus does decrease when the elevated temperature is sustained.
6. The mechanism for thermal wrinkling, once shrinkage has occurred, is governed by slippage and normal entry conditions. The slippage is the result of thermal expansion and modulus variation with temperature.
7. Wrinkling due to increase in temperature can be predicted using FEM modeling. If it can be shown that the maximum centerline stress value due to thermal expansion is greater than the stress value sustainable by friction between the web and roller, slippage will occur outwardly on the roller. This slippage will create negative steering angles. Then the edges will steer inward which will gather material in the center of the web. If the generated and sustainable stress values are above the

critical buckling stress, the gathered material is expected to generate wrinkles.

FUTURE WORK

The first part of this research looked at temperature rise behavior. It was observed that air entrainment has an effect on thermal resistance. Determining the contact resistance between the web and roller as a function of line speed and temperature would allow for a more accurate heat transfer model to be developed. This would lead to better predictions of web temperature as it transits the roller.

The second part of this research focused on wrinkling. The onset of wrinkling was studied by varying tension for a given temperature and line speed. Determining the onset of wrinkling by varying other parameters would lead to a better understanding of the conditions which lead to wrinkles occurring.

The last part of this research focused on predicting wrinkles trough model. This model has limitations stemming from the lack of friction in the model and the enforcing of normal entry. Using a better FEM software, such as ABAQUS, would allow for more accurate boundary and friction conditions to be applied. However for this to happen a more accurate modulus vs temperature curve needs to be determined as well.

REFERENCES

1. Good, J. K., Kedl, D. M., and Shelton, J. J., (1997) "Shear Wrinkling in Isolated Web Spans" Proceedings of the Fourth International Conference on Web Handling, Web Handling Research Center, Stillwater, Oklahoma

2. Good, J. K., and Straughan, P. (1999) "Wrinkling of Webs due to Twist", Proceedings of the Fifth International Conference on Web Handling, Web Handling Research Center, Stillwater, Oklahoma

3. Lightbourn, E. D. (1999) *Thermal Contact Resistance of Metal Roller to Plastic Web Interfaces*, M.Sc., University of Wisconsin-Madison

4. Incropera, Frank P, DeWitt, David P. (2007). Introduction to heat transfer. New York: Wiley.

5. Divakaruni, S. (2011), *Wrinkling of webs approaching heated rollers*, M.Sc., Oklahoma State University

6. Pagilla, P and Lu, Y, (2012) "Modeling of Temperature distribution in a Moving Web Transported over a Heat Transfer Roller", ASME 2012 5th Annual Dynamic Systems and Control Conference, Fort Lauderdale, Florida

7. Jones, D.P., McCann, M.J. and Abbot, S.J., (2011) "Web Tension Variations Caused by Temperature Changes and Slip on Rollers" Proceedings of the Eleventh International Conference on Web Handling, Web Handling Research Center, Stillwater, Oklahoma

8. Timoshenko, S. and Gere, J., (1961) Theory of Elastic Stability, 2nd Ed, McGraw-Hill, New York

9. Knox, K.L. and Sweeney, T.L., (1971) "Fluid Effects associated with Web Handling" Industrial Engineering Chemical Process Design Development, V10, N2, pp 201-205

10. DuPont Teijin Films. (2003) Mylar H-37232-3: Physical-Thermal Properties http://usa.dupontteijinfilms.com/informationcenter/downloads/Physical_And_Thermal_Properties.pdf

11. Segerlind LJ., (1984), Applied Finite Element Analysis, Sec 14.4. New York: Wiley;

12. ASTM Standard D1204-14, (2014), "Linear Dimensional Changes of Nonrigid Thermoplastic Sheeting or Film at Elevated Temperature," ASTM International, West Conshohocken, PA, 2014, DOI: 10.1520/D1204 www.astm.org

13. Calex Electronics Limited. Infrared Thermometry: Understanding and using the infrared Thermometer, http://www.calex.co.uk/downloads/application_guidance/understanding_and_using_ir.pdf

14. Shelton, J. J., (1968), *Lateral Dynamics of a Moving Web,* Order No. 6914333, Oklahoma State University http://search.proquest.com/docview/302382879?accountid=4117

15. Good, J. K., Beisel, J. A., and Yurtcu, H., (2009), "Predicting Web Wrinkles on Rollers" Proceedings of the Tenth International Conference on Web Handling, Web Handling Research Center, Stillwater, Oklahoma

16. Jones, D. P. (2001), "Traction in Web Handling: A Review," Proceedings of the Sixth International Conference on Web Handling, Ed. Good, J. K., Oklahoma State University

17. Jones, D.P., McCann, M.J. and Bishop, C.A., (2013), "Wrinkle Initiation and Development in Heated Webs on Drums" Proceedings of the Twelfth International Conference on Web Handling, Web Handling Research Center, Stillwater, Oklahoma

APPENDIX I

EQUIPMENT SPECIFICATIONS

Data Logger Thermometer

MAKE	YCT
MODEL	YC-747UD
SERIAL	12030581

Used to collect and transmit roller and air temperature data from Type K thermo-couples to PC software via USB

Force Gauge

MAKE	SHIMPO
MODEL	FGE-50
SERIAL	E929H125

Used to measure force when determining coefficient of friction

Magnetic Protractor

MAKE Ace

Used to determine rotational position of IR Thermometer

IR Controller

MAKE	CHINO
MODEL	IR-GZ01N
SERIAL	L412YR064

Used to relay data from CHINO IR thermometer to PC via 4-20 mA analog output.

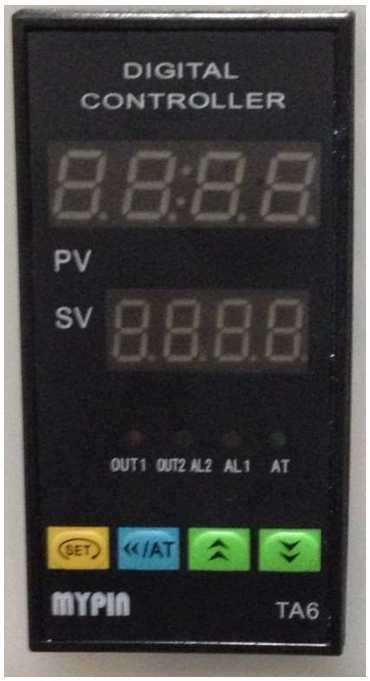

PID Controller

MAKE	MYPIN
MODEL	TA6-SNR+SSR

Used to control temperature of roller during temperature rise experiments. Controls Solid State Relay

Tachometer

MAKE	SHIMPO
MODEL	DT-105
SERIAL	30508902

Used to measure line speed

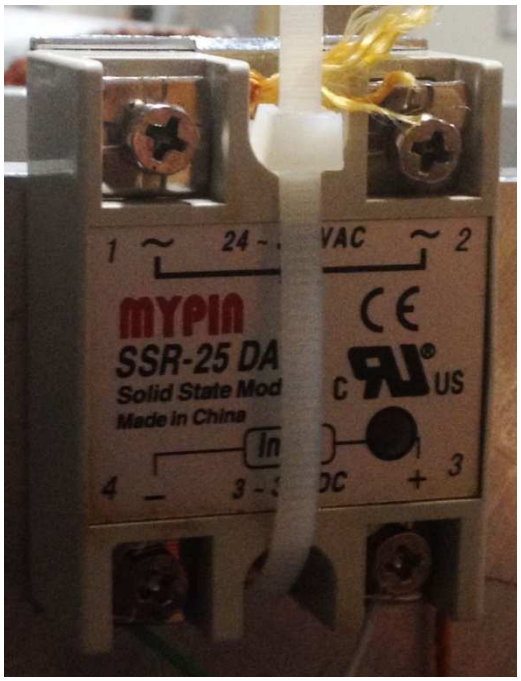

Solid State Relay

MAKE	MYPIN
MODEL	SSR-25 DA

Control by PID Controller. Used to control voltage across heating element in roller during temperature rise experiments

Variac Transformer

MAKE	POWERSTAT
MODEL	116

Used to control voltage across radiation heating elements during wrinkling experiments

Linear variable differential transformer

MAKE	OMEGA
MODEL	LD400-5
SERIAL	

Used during coefficient of thermal expansion test to measure displacement.

Infrared Thermometer

MAKE	CHINO
MODEL	IR-CANJCS
SERIAL	IA133N901

Used to measure temperature of polyester film during experiments

Environmental Chamber

MAKE	S.E.S. Inc
MODEL	RTT/6S
SERIAL	92055

Used to heat material sample during material properties tesing

Heating Cartridges

Cartridge Heater, High-Temperature, Standard Lead Cover, 3/8" Diameter, 8" Length, 600 Watts, 120 volts

Used to heat roller surface via radiation during wrinkling experiments

Heating element + Type K thermocouple

Used in conjunction with PID controller to heat oil in roller during temperature curve experiment

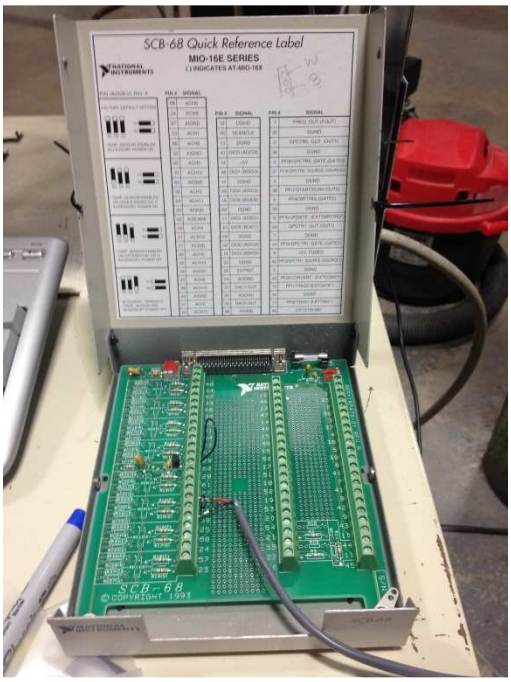

SCB-68 Analog DAQ

MAKE	Natl Instru
MODEL	MIO-16E
SERIAL	

Used to record 4-20 mA data from IR thermometer contoller

Force Transducer

MAKE	MAGPOWER
MODEL	CL250
SERIAL	120696005

Used to measure line tension

Web Guide

MAKE	FIFE
MODEL	SYMAT 25
SERIAL	2012563-00

Used to maintain lateral position of web before it transited the heated roller

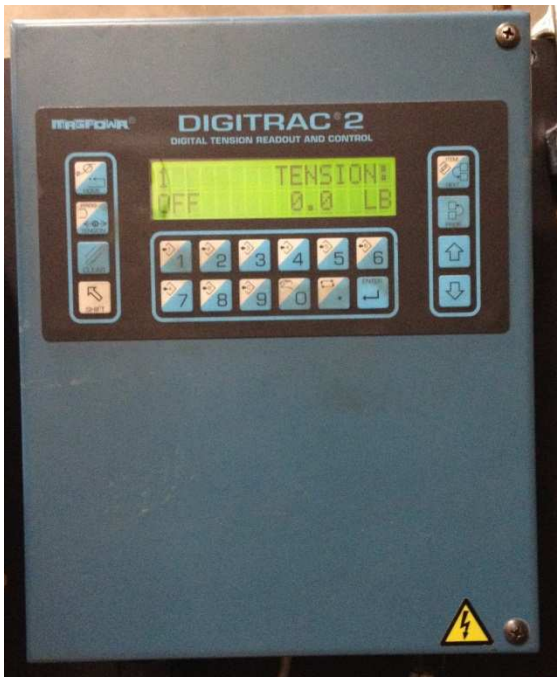

Tension Controller

MAKE	MAGPOWER
MODEL	DIGITRAC 2
SERIAL	

Used to set line tension

PLC

MAKE	Allen Bradley
MODEL	PowerFlex 700
SERIAL	

Used to set line speed

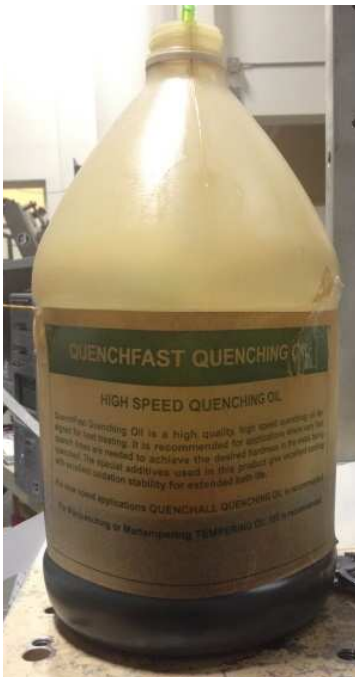

Quenching Oil, Motor Oil Inc

MAKE Quenchfast
MODEL
SERIAL

Used as a conduction medium in the heated roller.

APPENDIX II

COSMOS/M INPUT

```
C* Define Surfaces
SF4CORD,1,0,-3,0,0,3,0,-22,3,0,-22,-3,0;
SF4CORD,2,18.5,-3,0,18.50,3,0,8.5,3,0,8.5,-3,0;
SF4PT,3,8,7,2,1,0;
C* Define Elements and material
EGROUP,1,SHELL4,2,0,0,0,0,0,0,0;
RCONST,1,1,1,7,0.00092,0,0,0,0,0,1e-008;
MPROP,1,ALPX,.000025;
MPROP,1,NUXY,0.38;
C* Declare Temperature curve
CURDEF,TEMP,3,1,0,1,1,10,;
C* Declare Modulus
MPROP,1,EX,1.0;
C* Create Mesh
M_SF,2,2,1,4,18,30,1,1;
M_SF,3,3,1,4,18,34,1,1;
M_SF,1,1,1,4,18,66,1,1;
NMERGE,1,2600,1,0.0001,0,1,0;
NCOMPRESS,1,2600
C* Declare C1 curve
CURDEF,TIME,1,1,0,0,1,0.1;
C* Define MD Pressure
PCR,2,-1,2,1,-1,1;
PCR,5,1,5,1,1,1;
C* Constraints
DND,1283,UX,0,1283,1, UY;
DND,48,UY,0,67,19, ;
DND,2423,UY,0,2442,19, ;
DSF,1,UZ,0,3,1,;
C* Declare C2 curve
CURDEF,TIME,2,1,0,0,1,0.1,;
C* Define edge Displacements
DCR,4,UY,-1,4,1, ;
DCR,8,UY,-1,8,1, ;
DCR,10,UY,-1,10,1, ;
DCR,3,UY,1,3,1, ;
DCR,7,UY,1,7,1, ;
DCR,9,UY,1,9,1, ;
C* Declare C3 curve
CURDEF,TIME,3,1,0,0,1,0.1,;
VIEW,1,2,3,0;
PSCAN;
PSCAN;
C* Define temperature change at Nodes
NTND,1236,0,2489,1;
NTND,1217,28,1235,1;
NTND,1198,158,1216,1;
NTND,1179,206,1197,1;
NTND,1160,220,1178,1;
NTND,1141,225,1159,1;
```

NTND,1122,227,1140,1;
NTND,1103,228,1121,1;
NTND,1084,228,1102,1;
NTND,1065,228,1083,1;
NTND,1046,228,1064,1;
NTND,1027,228,1045,1;
NTND,1008,228,1026,1;
NTND,989,228,1007,1;
NTND,970,228,988,1;
NTND,951,228,969,1;
NTND,932,228,950,1;
NTND,913,228,931,1;
NTND,894,228,912,1;
NTND,875,228,893,1;
NTND,856,228,874,1;
NTND,837,228,855,1;
NTND,818,228,836,1;
NTND,799,228,817,1;
NTND,780,228,798,1;
NTND,761,228,779,1;
NTND,742,228,760,1;
NTND,723,228,741,1;
NTND,704,228,722,1;
NTND,685,228,703,1;
NTND,666,228,684,1;
NTND,647,228,665,1;
NTND,628,228,646,1;
NTND,609,228,627,1;
NTND,590,228,608,1;
NTND,571,228,589,1;
NTND,552,225,570,1;
NTND,533,222,551,1;
NTND,514,219,532,1;
NTND,495,216,513,1;
NTND,476,213,494,1;
NTND,457,210,475,1;
NTND,438,207,456,1;
NTND,419,204,437,1;
NTND,400,201,418,1;
NTND,381,198,399,1;
NTND,362,195,380,1;
NTND,343,192,361,1;
NTND,324,189,342,1;
NTND,305,186,323,1;
NTND,286,183,304,1;
NTND,267,180,285,1;
NTND,248,177,266,1;
NTND,229,174,247,1;
NTND,210,171,228,1;
NTND,191,168,209,1;

```
NTND,172,165,190,1;
NTND,153,162,171,1;
NTND,134,159,152,1;
NTND,115,156,133,1;
NTND,96,153,114,1;
NTND,77,150,95,1;
NTND,58,147,76,1;
NTND,39,144,57,1;
NTND,20,141,38,1;
NTND,1,138,19,1;
C* Define variables
PARASSIGN,DT,REAL,0.5;
PARASSIGN,THICK,REAL,0.00092;
PARASSIGN,PLI,REAL,1.0;
C* Define C1 curve
CURDEF,TIME,1,1,0,0,0.5,0.25*PLI/THICK,1.0,0.5*PLI/THICK,1.50,0.75*PLI/T
HICK,2.0,0.99*PLI/THICK,10.0,PLI/THICK,;
C* Define C2 curve
CURDEF,TIME,2,1,0,0,2.0,0,4.0,0.99*3*0.38*PLI/(THICK*800000),10,3*0.38*P
LI/(THICK*800000),;
C* Define C3 curve
CURDEF,TIME,3,1,0,0,4.0,0,8.0,0.5,10.0,1.0,;
C* Define Temperature curve
CURDEF,TEMP,3,1,0,800000,103,511000,230,146000,;
TIMEs,0,10,DT;
C* Define convergence Criterion
A_NONLINEAR,S,1,1,20,0.01,0,T,0,0,1e+010,0.001,0.01,0,1,0,0;
R_NON
C* Plot sigma Y
ACTSTR,10/DT,SY,1,1,0,0
STRPLOT,0,1,2600,1,0,24.2792
LSECPLOT,1226,580,10,10,;
```

VITA

Ryan Oliver

Candidate for the Degree of

Master of Science

Thesis: DETERMINATION OF THE TEMPERATURE PROFILE AND WRINKLING BEHAVIOR OF WEBS TRANSITING HEATED ROLLERS

Major Field: Mechanical Engineering

Biographical:

Born in Vinita, Oklahoma in 1986.
Raised in Bartlesville, Oklahoma from 1990 to 2005
Resided in Wichita, Kansas from 2009 to 2012

Education:

Completed the requirements for Master of Science in Mechanical Engineering at Oklahoma State University, Stillwater, Oklahoma in May, 2014.

Completed the requirements for Bachelor of Science in Mechanical Engineering at Oklahoma State University, Stillwater, Oklahoma in May, 2009.

Experience:

Graduate Research Assistant, Mechanical & Aerospace Engineering Department, Oklahoma State University, Aug 2012 to Present

Graduate Teaching Assistant, Mechanical & Aerospace Engineering Department, Oklahoma State University, Aug 2012 to Present

Structural Analyst, Spirit AeroSystems, Wichita, KS, June 2009 to July 2012